12

ORIENTATION SELECTIVITY AND ITS MODULATION BY LOCAL AND LONG-RANGE CONNECTIONS IN VISUAL CORTEX

DAVID SOMERS

Department of Psychology, Boston University, Boston, Massachusetts

VALENTIN DRAGOI AND MRIGANKA SUR

Department of Brain and Cognitive Sciences, Massachusetts Institute of Technology, Cambridge, Massachusetts

OVERVIEW AND INTRODUCTION

Orientation selectivity of neurons in the primary visual cortex (V1) is one of the most thoroughly investigated receptive field properties in all of neocortex; however, its underlying neural mechanisms are still debated (see Das 1996; Sompolinsky and Shapley, 1997; Ferster and Miller, 2000). The earliest and simplest proposal for the generation of orientation selectivity was made by Hubel and Wiesel (1962). They proposed that a cortical simple cell receives input from a row of neurons in the lateral geniculate nucleus (LGN) whose receptive fields are aligned along the axis of orientation of the cortical receptive field (see Fig. 8-1 in Chapter by Reid et al.). This feedforward model, which postulates essentially lin-

ear summation of geniculate inputs, has had substantial experimental support (see for a recent review, Ferster and Miller, 2000).

At the same time, several kinds of evidence suggest that such a model does not capture the nonlinear complexity of cortical receptive fields and responses. In particular, V1 cells exhibit three significant kinds of nonlinear summation. First, the orientation selectivity of cortical cells is remarkably independent of stimulus contrast or the level of afferent drive. A purely feedforward model would predict that orientation tuning would broaden as contrast increases. Additions to the feedforward model have therefore been required. One proposal is that contrast gain control occurs by pooling the activity of cortical neurons and dividing or normalizing the geniculate input (Albrecht and Geisler, 1991; Heeger, 1992). Although recent evidence indicates that cortical neurons can exhibit the large changes in conductance that are required for such divisive normalization (Borg-Graham et al., 1998; Hirsch et al., 1998), the time course of changes is too brief for them to play a meaningful role in contrast gain control.

A second nonlinear feature of cortical cell responses is that they integrate inputs from a wide region of space that extends beyond the classical receptive field: stimuli in the receptive field surround can either enhance or suppress responses to stimuli in the receptive field center (Knierim and Van Essen, 1992; Grinvald et al., 1994; Sillito et al., 1995). We and others have shown that the effect of the surround on the center depends critically on the level of center drive (Toth et al., 1996; Sengpiel et al., 1997, 1998; Polat et al., 1998). Furthermore, stimulating the surround with stimuli that have a significantly different orientation than the cell's preferred orientation can enhance responses to optimally oriented center stimuli and generate supraoptimal responses (Sillito et al., 1995; Levitt and Lund, 1997). Third, orientation selectivity is not a static feature of V1 cells but can be altered dynamically by spatial and temporal context. For instance, adapting a cell with a stimulus of a given orientation causes a short-term change in the cell's preferred orientation (Dragoi et al., 2000). Responses on the flank of the tuning curve near the adapting orientation are suppressed, whereas responses on the far flank are actually enhanced, leading to a shift in orientation preference away from the adapting orientation. Such active nonlinear dynamics of orientation tuning are consistent with a progressive evolution of orientation tuning in V1 neurons observed on a rapid time scale using reverse correlation techniques (Ringach et al., 1997). More generally, altering the balance of excitation and inhibition in cortical columns alters the orientation tuning of adjacent columns (Toth et al., 1997a).

In this review, we argue that a model that takes into account not only thalamocortical excitation but also intracortical excitation between neurons in a cortical local circuit provides a fuller explanation of orientation selectivity. We have demonstrated that such a model provides a natural explanation for the contrast invariance of orientation tuning (Somers et al., 1995a). We summarize our model later and address some recent data that appear to contradict the model or support it. By adding long-range excitatory connections to neurons that are locally connected, we

have shown that the paradoxical enhancement/suppression of center responses by surround stimulation can be explained (Somers et al., 1998). Such spatial context effects are actually part of a broader range of spatial receptive field dynamics governed by stimulus contrast, including length summation in receptive fields and supersaturation of responses. Next we describe the effects of long-range connections on local recurrent networks. Recurrent connections between excitatory neurons alone cannot explain supraoptimal responses accompanying surround stimulation at nonoptimal orientations. We have shown that recurrent connections between inhibitory neurons provide a sufficient explanation for this phenomenon (Dragoi and Sur, 2000), and we summarize the model. Finally, we have recently described the temporal dynamics and short-term plasticity of orientation tuning in V1 neurons following adaptation to oriented stimuli (Dragoi et al., 2000). These data provide strong support for the hypothesis that recurrent excitation and inhibition between local circuit neurons mediate orientation tuning. Together, these models and results provide a unifying explanation for orientation selectivity and for several of the key nonlinear phenomena that accompany orientation tuning—phenomena that are beyond the purview of feedforward models alone.

CONTRIBUTIONS OF LOCAL CORTICAL EXCITATION TO THE GENERATION OF ORIENTATION SELECTIVITY: THE EMERGENT MODEL

INTRODUCTION

Models of visual cortical orientation selectivity can be broadly divided into three categories: feedforward, inhibitory, and recurrent excitatory (Fig. 12-1). In feedforward models, all first-order cortical neurons receive converging input from a population of LGN neurons whose receptive fields are aligned in strongly oriented fashion in visual space. The bandwidth or sharpness of a cortical cell's orientation tuning is determined by the aspect ratio of its LGN projection. Many inhibitory models use a mild feedforward bias to establish the initial orientation preference of cortical neurons and inhibitory inputs—from cortical neurons preferring different orientations—to suppress nonpreferred responses. In recurrent models, cortical excitation among cells preferring similar orientations, combined with iso-orientation inhibition from a broader range of orientations, integrates and amplifies a weak thalamic orientation bias, which is distributed across the cortical columnar population. In this section we present our emergent model, which was one of the first recurrent models of orientation selectivity (Somers et al., 1995a; Ben-Yishai et al., 1995). Subsequently, a significant number of models have incorporated similar principles and in some cases expanded or refined these ideas (Troyer et al., 1998; McLaughlin et al., 2000; Pugh et al., 2000; Chance et al., 1999).

Feedforward models have received renewed experimental support since our original model was published (Ferster et al., 1996; Reid and Alonso, 1995; Chung

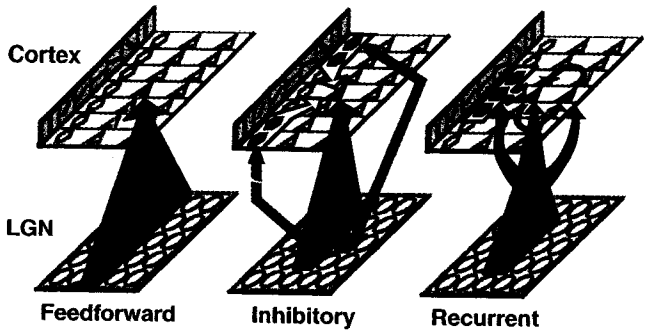

FIGURE 12-1. Models of visual cortical orientation selectivity. In feedforward models all "first-order" cortical neurons (triangle = excitatory, hexagon = inhibitory) receive converging input (gray arrow) from a population of LGN neurons that cover a strongly oriented region of visual space. A cortical cell's orientation tuning bandwidth is determined by the aspect ratio of its LGN projection. Many inhibitory models use a mild feedforward bias and use inhibitory inputs (white arrows), from cortical neurons preferring different orientations, to suppress nonpreferred responses. Here, we present a model in which recurrent cortical excitation (black arrows) among cells preferring similar orientations, combined with iso-orientation inhibition from a broader range of orientations, integrates and amplifies a weak thalamic orientation bias.

and Ferster, 1998; Anderson et al., 2000); however, problems linger with feedforward models (Ringach et al., 1997; Gardner et al., 1999). The key idea of feedforward models, that cortical neurons obtain orientation selectivity from elongated patterns of converging LGN inputs (Fig. 12-1 left) (Hubel and Wiesel, 1962; Ferster, 1987), is supported *qualitatively* by experiments. Thalamic ON cells (or OFF cells) are generally in close spatial register with the ON subfields (or OFF subfields) of cortical simple cells to which they provide input (Reid and Alonso, 1995). On average, cortical simple cell subfields are elongated along an axis parallel to the preferred response orientation (Jones and Palmer, 1987; Chapman et al., 1991). But for many simple cells, subfield length-to-width ratios (aspect ratios) are *quantitatively* insufficient to account for the sharp orientation selectivity exhibited (Watkins and Berkley, 1974; Jones and Palmer, 1987). Reports of low mean aspect ratios (Chapman et al., 1991; Pei et al., 1994; Reid and Alonso, 1995) are also inconsistent with feedforward models of orientation selectivity. Weakly biased feedforward inputs can be sharpened by using high firing thresholds (the "iceberg" effect, Creutzfeldt et al., 1974b), but this mechanism incorrectly predicts broadening of orientation tuning with increasing stimulus contrast (Sclar and Freeman, 1982; Wehmeier et al., 1989). Pure feedforward models also cannot account for the loss of orientation selectivity under iontophoresis of bicuculline, a $GABA_A$ antagonist that reduces inhibition over a localized population of cortical neurons (Sillito, 1975; Tsumoto et al., 1979; Sillito et al., 1980) (see Chapter 11).

Mechanisms that use shunting ("divisive") inhibition (e.g., Koch and Poggio, 1985; Carandini and Heeger, 1994) or hyperpolarizing ("subtractive") inhibition at

nonpreferred orientations (Fig. 12-1 middle) (e.g., Wehmeier et al., 1989; Worgotter and Koch, 1991) can sharpen tuning in cells which have mildly oriented thalamocortical inputs; such models can also produce contrast-invariant orientation tuning and can account for bicuculline-induced tuning loss. However, inhibitory models are inconsistent with other experimental data. Although shunting inhibition has recently been rediscovered in cortex (Borg-Graham et al., 1998; Hirsch et al., 1998), it occurs only very transiently and appears insufficient to account for orientation selectivity (Douglas et al., 1988; Berman et al., 1991; Dehay et al., 1991; Ferster and Jagadeesh, 1992; Anderson et al., 2000). Inhibitory postsynaptic potentials (IPSPs) are evoked strongly by stimuli presented at the preferred orientation, whereas stimuli at cross-orientations evoke weak IPSPs (Ferster 1986; Douglas et al., 1991). Such inhibitory tuning conflicts with cross-orientation inhibitory models (Bishop et al., 1973; Morrone et al., 1982), and strong iso-orientation suppression poses problems even for models that use other forms of hyperpolarizing inhibition to sharpen thalamocortical input (e.g., Worgotter and Koch, 1991). Furthermore, results from our laboratory conflict with all orientation models that rely heavily on direct inhibitory input. Intracellular blockade of inhibition had *negligible* effect on sharpness of orientation tuning of blocked cells (Nelson et al., 1994). These results also appear to conflict with reports that orientation tuning can be abolished by bicuculline-induced extracellular inhibitory blockade (Sillito et al., 1980; Nelson, 1991) (see Chapter 11).

In this section, we demonstrate that this apparent paradox can be resolved by considering the effects the two inhibitory blockades have on the tuning of cortical excitatory inputs. Our computer simulations also demonstrate that local, recurrent cortical excitation can generate sharp, contrast-invariant orientation tuning in circuits that have strong iso-orientation inhibition and weakly oriented thalamocortical excitation (Fig. 12-1 right). This model primarily addresses the circuitry within a single cortical "hypercolumn"; effects of adding long-range cortical connections to this circuitry are addressed in the next section.

KEY ASSUMPTIONS OF THE MODEL

Although the model incorporated significant biological detail, only three assumptions were critical to this model. First, converging LGN inputs must provide *some* orientation bias at the columnar population level. Consistent with experiment (Creutzfeldt et al., 1974a; Watkins and Berkley, 1974; Jones and Palmer, 1987; Chapman et al., 1991; Pei et al., 1994), this bias may be weak and distributed across a population with many cells that receive unoriented input. The second assumption of the model—that local (< 1 mm horizontal distance) intracortical inhibitory connections must arise from cells with a broader distribution of orientation preferences than do intracortical excitatory connections—differs from prior inhibitory models in that it is consistent with experimental evidence for strong iso-orientation inhibition (Ferster, 1986; Douglas et al., 1991; Anderson et al., 2000). Narrowly tuned iso-orientation excitation and more broadly tuned iso-

orientation inhibition can be realized by a simple difference-of-gaussians like structure in the orientation domain. This idea is supported by cross-correlation data (Hata et al., 1988; Michalski et al., 1983) and is consistent with a key hypothesis of many models of the development of orientation selectivity (e.g., Rojer and Schwartz, 1990; Miller, 1992, 1994; Swindale, 1992; Grossberg and Olson, 1994). The original model (Somers et al., 1995a) used a somewhat large difference in the input ranges of excitatory and inhibitory inputs. Below (Fig. 12-4C) we show that the inhibitory inputs can be much narrower than we originally claimed; inhibitory inputs need be only slightly broader than excitatory cortical inputs. This seems consistent with recent experimental reports (Anderson et al., 2000). The final assumption is that cortical inhibition must approximately balance cortical excitation. Too much inhibition produced low response rates and too little inhibition permitted nonselective amplification of all stimulus responses. However, many sets of parameters satisfied the "balance" requirement. This hypothesis is consistent with reports that excitatory postsynaptic potentials (EPSP) and inhibitory postsynaptic potentials (IPSP) strengths roughly covary across orientations (Ferster, 1986; Douglas et al., 1991; however, see Pei et al., 1994 for a differing view). Balanced cortical excitation and inhibition have also been invoked by computational models of cortical response variability (Softky and Koch, 1993; Shadlen and Newsome, 1994).

MODEL STRUCTURE AND IMPLEMENTATION

The model addresses the generation of orientation selectivity in cortical neurons that receive direct thalamic input. The circuit represents layer IV simple cells that lie under a 1700 μm by 200 μm patch of visual cortical area 17 of the cat. This small cortical area contains orientation columns representing a full set of preferred orientations (e.g., a hypercolumn), as well as neighboring columns. The model implemented 2205 cortical neurons, of which 20% were inhibitory and the rest excitatory (Gabbott and Somogyi, 1986). In total, the network contained more than 180,000 synapses.

Cortical neurons were organized into 21 orientation columns, spanning the length dimension of the cortical patch. An initial, but weak orientation structure was generated in cortex by providing orientation-biased converging LGN input to each cortical column. Simple cell subfield aspect ratios varied between 1:1 (unoriented) and 3:1 (moderately oriented). Cortical neurons received synaptic inputs from lateral geniculate (excitatory), cortical excitatory, and cortical inhibitory neurons. The model assumed LGN inputs contribute 20% of all synapses, and that cortical excitatory and inhibitory neurons, respectively, receive 20% and 10% of their synapses from cortical inhibitory neurons. Model cortical excitatory cells provided 60% and 70% synapses onto excitatory and inhibitory neurons, respectively.

To generate iso-orientation excitation and inhibition, cortical excitatory and inhibitory inputs were chosen from normal distributions, each with maximal connectivity probability *within* the cortical column of the postsynaptic cell. Inhibitory

inputs were drawn from a broader range of orientations than the excitatory inputs. Inhibitory inputs had a range of ± 60° (~± 350 μm), whereas excitatory inputs had an effective range of ± 15° (~± 100 μm). We show later in this section (see Fig. 12-4c) that inhibitory inputs need be only modestly broader than cortical excitatory inputs to provide this degree of cortical sharpening effect. Effects of long-range connections are addressed in the next section.

Excitatory and inhibitory cortical neurons were modeled separately using experimentally reported input resistances, membrane time constants, and firing characteristics of regular-spiking (RS) and fast-spiking (FS) neurons (Connors et al., 1982; McCormick et al., 1985). Each cortical neuron was modeled as a single voltage compartment in which the membrane potential, V, was given by:

$$C_m\, dV_i/dt = -\sum_{j=1}^{k} g_{ji}\,(t - t_{ji})\,(V_i\,(t) - E_{Excit}) - \sum_{j=k+1}^{k+l} g_{ji}\,(t - t_{ji})\,(V_i\,(t) - E_{Inhib})$$

$$- g_{Leak}\,(V_i\,(t) - E_{Leak}) - g_{AHP}\,(t - t_{spike})\,(V_i\,(t) - E_{AHP})$$

where the synaptic conductances generated at each postsynaptic cell i by the spiking of each presynaptic cell j (excitatory if j <= k; inhibitory if k < j <= l) were given by:

$$g_{ji}\,(t) = \bar{g}_{ji} \sum_{p}^{S_j} (t - t_p)\,(e/\tau_{peak})\,\exp\,[-(t - t_p)/\tau_{peak}]$$

where t_{ji} and $\bar{g}_{ji}$ describe the delay and maximal conductance change produced for the synapse between cell j and cell i. The numbers of excitatory and inhibitory synapses received by cell i were k and l, respectively. AMPA receptor-mediated excitatory synaptic effects and $GABA_A$ receptor-mediated synaptic inhibitory effects were implemented as linear conductance changes. After-hyperpolarization effects were spike-triggered (with delay t_{spike} = 1 ms). In general, parameter choices were very conservative; see Somers et al. (1995a) for further discussion.

MODEL PERFORMANCE

Response Behavior

Orientation tuning properties of the model were thoroughly investigated. Both excitatory and inhibitory neurons were sharply selective. Mean HW tuning of excitatory cells was 17.1° ± 0.6° (SD), and mean HW tuning of inhibitory cells was 20.5° ± 0.7° (SD). The sharpness of tuning is consistent with typical physiological values for cortical simple cells (Watkins and Berkley, 1974; Orban, 1984). Figure 12-2A displays a simulated intracellular trace of a typical model cortical excitatory cell in response to flashed bar stimuli oriented at 0°, 22.5°, 45°, and 90°. As is true for all cells in the column, this cell is sharply selective for the 0° stimulus.

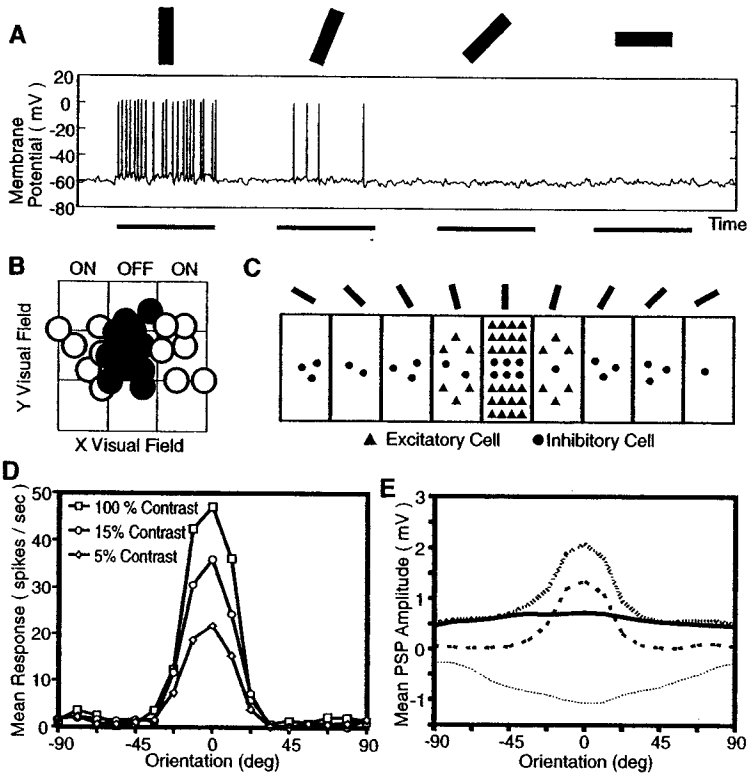

FIGURE 12-2. Response of a cell selective for 0° stimuli. **(A)** Simulated intracellular trace from one cell in the model network in response to flashed dark bars oriented at 0°, 22.5°, 45°, and 90°. Black bars on time axis indicate 500 msec stimulus presentation. **(B)** Thalamic and **(C)** cortical input fields of this cell. ON (white) and OFF (black) thalamic subfields exhibited only a mild orientation bias for 0° stimuli. Cortical excitatory (triangles) and inhibitory (circles) inputs arose most densely from cells within the 0° column. Inhibitory distribution was broader than the excitatory distribution. **(D)** As contrast increased, peak response increased but selectivity did not broaden. **(E)** Postsynaptic potentials evoked in the example cell by thalamic excitatory (solid), cortical excitatory (thick dashed), and cortical inhibitory (thin dashed) synaptic inputs.

Sharpness of orientation selectivity remained approximately constant across stimulus contrasts values. As contrast increased, peak responses increased but selectivity did not broaden. This contrast-invariance of orientation tuning in the model replicates experimental findings (Sclar and Freeman, 1982). Figure 12-2D displays orientation-response curves at three different contrasts for an example cell.

The mechanisms underlying orientation tuning of the model were investigated by measuring the postsynaptic potentials (PSPs) contributed by different synaptic input sources. Both excitatory (EPSP) and inhibitory (IPSP) PSPs were strongest

at the preferred orientation (Fig. 12-2E). Notably, stimulus-evoked IPSPs (in excess of spontaneous levels) were, on average, 8.3 times as strong for the preferred orientation as for the orthogonal or cross-orientation (90°) stimulus. These PSP tuning properties of the model are consistent with intracellular reports of weak cross-orientation IPSPs and strong iso-orientation IPSPs (Ferster, 1986; Douglas et al., 1991).

In the model, the EPSP tuning resulted from a combination of broadly tuned thalamocortical input and sharply tuned corticocortical excitation. Broad tuning of thalamocortical input resulted from the low length to width ratios of the (regions of thalamic convergence onto) cortical subfields (Fig. 12-2C). Sharp tuning of cortical EPSPs reflected input from well-tuned cortical excitatory cells with similar orientation preferences. Cortical inhibitory inputs were also drawn most heavily from within the preferred orientation column (Fig. 12-2B), and these cells were also well tuned. Cortical inhibitory inputs were drawn from a broader range of orientations than cortical excitatory inputs; therefore cortical inhibition was more broadly tuned than cortical excitation. We show later (see Fig. 12-4C) that the critical orientation sharpening property can be obtained with much narrower cortical inhibition than was used here. Net EPSPs and IPSPs were evoked over a similar range of orientations. EPSP and IPSP tuning curves differed primarily in their slope at oblique orientations.

Claim of Emergence, Speed of Emergence

The PSP records revealed that cortical excitatory inputs were the source of the largest and best-tuned orientation signal (see Fig. 12-4). Therefore, cortical excitation was the leading cause of sharp orientation selectivity. This finding may appear paradoxical, as sharp tuning of cortical neurons was both the "effect" and the "cause" of the effect; however, in a feedback circuit such an explanation is not tautological. Rather, it implies that the effect is an *emergent* property of the recurrent circuitry.

Because sharp orientation selectivity resulted from cortical feedback, rapid sharpening of EPSP tuning can be observed in the model's intracellular records at the beginning of a response. Broadly tuned thalamocortical EPSPs are quickly joined by sharply tuned intracortical EPSPs. Pei et al. (1994) reported a similar sharpening in PSP tuning in vivo. Similar rapid sharpening effects have also been reported in anesthetized and awake monkeys (Ringach et al., 1997; Dragoi et al., 1999) and in optical recordings of cats (Shoham et al., 1999). However, the temporal evolution of tuning is less apparent in the model's extracellular traces. For nearly all model cells, sharp orientation selectivity emerged by the first or second spike of the response. This is consistent with experimental reports (Vogels and Orban, 1991). Because of the integrative properties of membranes, response latencies were generally shortest for preferred stimuli (c.f., Dean and Tolhurst, 1986). This "head-start" for preferred orientations likely contributed to the rapid emergence of sharp tuning in the model. Although not incorporated in this model, brief but strong shunting inhibition that has recently been observed might also

play an important role in controlling transient responses (Borg-Graham et al., 1998; Hirsch et al., 1998).

Analysis of Orientation Tuning

To investigate further the mechanisms underlying orientation selectivity in the model, the maximal synaptic conductances (strengths) for all cortical inhibitory and/or cortical excitatory synapses were manipulated. The precise set of network connections, however, was otherwise unaltered. Inactivation of cortical excitatory and cortical inhibitory synapses revealed tuning effects of the converging thalamocortical inputs. LGN inputs alone generated broad tuning with a large variance in tuning across the population of cortical neurons (Fig. 12-3a). The most sharply tuned neuron in the feedforward circuit was more broadly tuned than the most broadly tuned cell in the full network. This demonstrates that the role of intracortical excitation was not simply to "convey" sharp tuning from a few cells, which receive highly oriented thalamocortical inputs, to other neurons.

Simulations were also performed on a variation of the model with normal intracortical inhibition and normal thalamocortical excitation, but inactivated intracortical excitation. This network ("inhib 1") exhibited tuning sharper than that of the feedforward network, but significantly broader than that of the full feedback network. Mean excitatory cell HW tuning was 38.4° ± 22.7° SD. This network also exhibited lower response rates than either the full network or the feedforward network. Mean peak response of excitatory neurons was 9.8 spikes/sec ± 2.3 sp/s SD. (compared with 47 sp/s for the full network). The tuning advantage of this inhibitory network over the feedforward network can be attributed to an "iceberg" effect; relatively unoriented hyperpolarizing inhibition is similar to raising the threshold. To investigate more thoroughly iceberg-type effects in this model, the maximal inhibitory synaptic conductances were doubled and cortical excitation remained. This ("inhib 2") network exhibited only a mild improvement in orientation tuning over the "inhib 1" network. The increase in inhibition also resulted in a further reduction of response rates. In contrast, the full recurrent network exhibited both physiologically sharp orientation tuning and robust responses. These results demonstrate that the orientation tuning properties of the model cannot be accounted for by either the thalamocortical or intracortical inhibitory connections it utilized. Thus these results demonstrate the utility of local, recurrent, cortical excitatory connections in the generation of sharp orientation selectivity by the model.

To explore further the robustness of the model, orientation behavior was explored for a broad range of cortical excitatory and inhibitory synaptic strengths. Mean response and orientation tuning of the summed responses of all excitatory neurons in the 0° column were measured for each parameter set (Fig. 12-3b). This analysis revealed a diagonal band of "balanced" excitatory and inhibitory strengths that yield both sharp tuning and robust responses. In the region below this diagonal, inhibition dominated, causing reduction of response. In the region above the diagonal band, excitation dominated, causing nonselective amplifica-

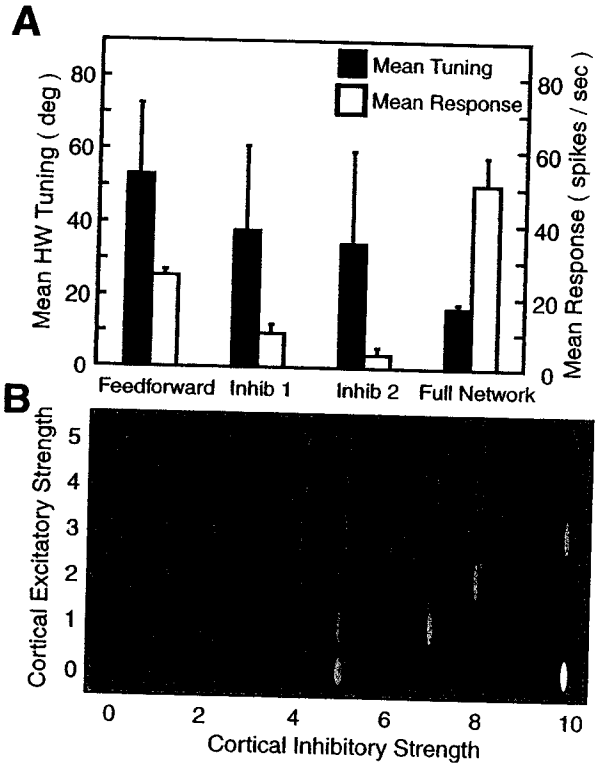

FIGURE 12-3. (A) Recurrent network tuning properties compared to those of the network components. (B) Sensitivity of the model to cortical excitatory and inhibitory strengths. Average peak response (indicated by symbol shading; darker = stronger response) and orientation tuning bandwidth (indicated by symbol shape; more elliptic = sharper tuning) of averaged responses of cortical excitatory neurons, for different cortical synaptic strengths (in nS). The model exhibited sharp orientation tuning and strong responses provided that cortical excitation and inhibition were approximately balanced. The region between the two lines defines the region of parameter space that satisfied this "balance" requirement. Where inhibition dominated, response rates fell; where excitation dominated, tuning broadened.

tion of *all* responses and thus a broadening of tuning. Explorations of networks with different spatial spreads of cortical connections also revealed similar (but shifted) diagonal bands of "balanced" excitation and inhibition for which sharp tuning was observed.

Additional analysis was performed to further illuminate the mechanism by which this model achieved sharp orientation tuning and robust responses (despite utilizing poorly oriented thalamocortical inputs and iso-orientation inhibition). Figure 12-4A displays the mean orientation response curve for cells in the thalamocortical network and an example of a "desired" orientation response curve

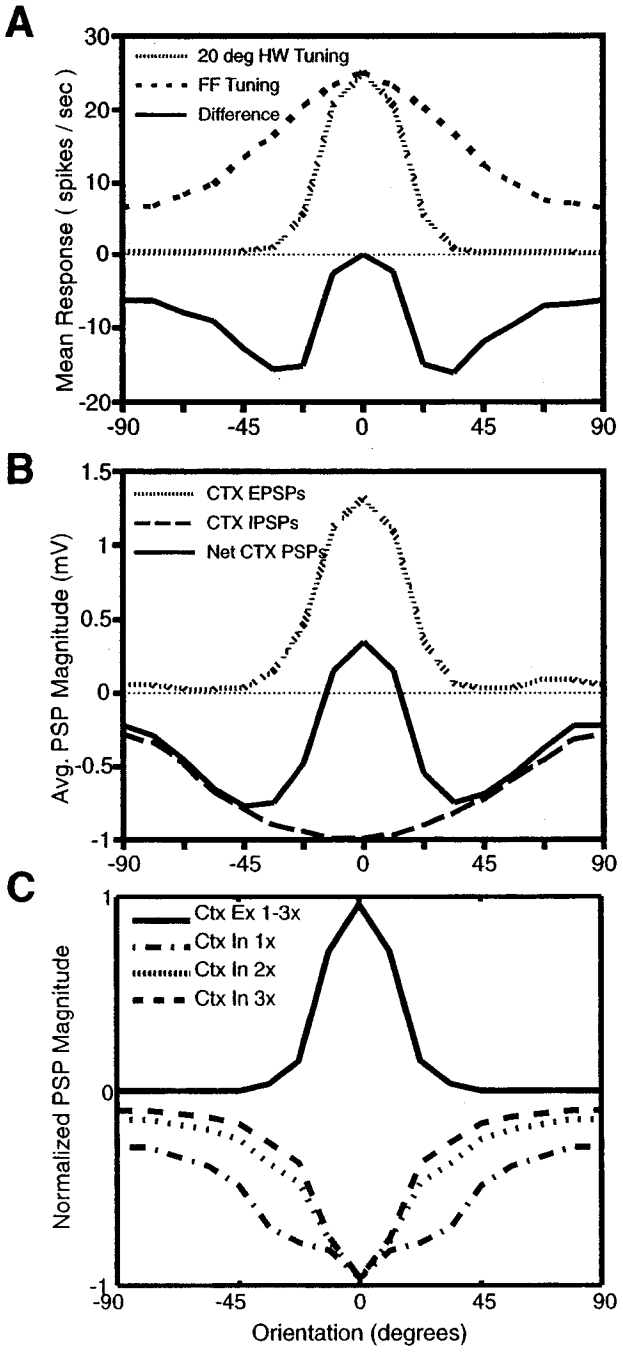
A
20 deg HW Tuning
FF Tuning
Difference
Mean Response (spikes / sec)
30
20
10
0
-10
-20
-90
-45
0
45
90
B
CTX EPSPs
CTX IPSPs
Net CTX PSP
Avg. PSP Magnitude (mV)
1.5
1
0.5
0
-0.5
-1
-90
-45
0
45
90
C
Ctx Ex 1-3x
Ctx In 1x
Ctx In 2x
Ctx In 3x
Normalized PSP Magnitude
1
0
-1
-90
-45
0
45
90
Orientation (degrees)

with HW tuning of 20° (typical tuning for simple cells; Orban, 1984). The desired tuning curve was scaled so that the peak responses of the two curves were equal. To achieve 20° HW tuning, the difference between the desired orientation tuning response and the thalamocortical response must be provided by cortical inputs. Therefore, the difference curve (Fig. 12-4A) reveals the shape of orientation tuning of the net cortical contribution required to achieve sharp orientation selectivity. This curve indicates that net cortical inhibition should be strongest at approximately 20° to 40° from the preferred orientation. Modest net cortical inhibition is required at the cross-orientation.

The net cortical tuning curve indicates that little or no iso-orientation inhibition is required; an iso-orientation specific increase in inhibition would both reduce responsiveness and broaden tuning. Since experimental intracellular recordings indicate that cortical inhibition is actually strongest at the iso-orientation (Ferster, 1986; Douglas et al., 1991; Anderson et al., 2000), the net cortical orientation tuning curve cannot be accounted for solely by the cortical inhibitory inputs. However, the net cortical curve *can* be matched by combination of somewhat broad iso-orientation cortical inhibition and iso-orientation cortical excitation. Figure 12-4B displays the average cortical excitatory and inhibitory inputs (PSPs) to excitatory cortical cells in the full model. The net cortical orientation tuning curve produced by their sum exhibits the same center-surround structure displayed in the difference curve of Fig. 12-4A.

This analysis demonstrates that narrowly tuned cortical excitation can provide the "missing link" between the combination of broadly tuned thalamocortical excitatory inputs and iso-orientation inhibitory inputs on the one hand and sharply tuned orientation output responses on the other hand. The "center-surround" orientation tuning mechanism described here can be generated by any of a family of pairs of excitatory and inhibitory cortical inputs in which excitation and inhibition are approximately balanced and inhibition is more broadly tuned than excitation.

FIGURE 12-4. Cortical requirements for sharp orientation selectivity. **(A)** Comparison of orientation responses produced by thalamocortical inputs alone (FF tuning) with typical physiological tuning (20° HW). The difference between these curves must be contributed by intracortical inputs. Note that net inhibition is most strongly required approximately 20° to 40° from the preferred orientation. **(B)** Average cortical PSPs received by excitatory cells in the 0° column. Narrow iso-orientation excitation and broader iso-orientation inhibition combined to yield "center-surround" cortical orientation tuning with net excitation in response to preferred stimulus orientations and net inhibition for nonpreferred stimuli. Net cortical tuning satisfied inhibitory requirements of the difference curve (in part A) and amplified preferred responses. **(C)** Family of cortical excitatory and inhibitory PSP curves that produce the net cortical PSP curve required in panel A. As the strength of net cortical excitation increases relative to net thalamocortical excitation, the shape of the required IPSP curve becomes narrower. Normalized curves are shown for net cortical EPSPs 1, 2, and 3 times net thalamocortical EPSPs (based on preferred orientation amplitude). Solid line shows a normalized EPSP curve (always the same shape). Broken lines shows IPSP curve for net cortical EPSPs 1,2, and 3 times as strong as net thalamocortical.

Such a family of balanced excitatory and inhibitory cortical inputs was generated in the model as stimulus contrast was varied. This family also admits much more narrowly tuned cortical inhibitory inputs (Fig. 12-4C) than we proposed earlier. As the size of the cortical inputs increases relative to the size of the thalamocortical inputs, the shape of the "required" inhibitory curve narrows substantially. If the net cortical excitatory inputs at the preferred orientation are two or three times as strong as the net thalamocortical inputs at the preferred orientation, the cortical inhibitory input curve narrows to be very similar to the cortical excitatory curve. The exact ratio of thalamocortical and intracortical input strengths is still under experimental investigation. Individual thalamocortical synapses appear to be stronger than individual intracortical excitatory synapses (Stratford et al., 1996; Gil et al., 1999), but cortical excitatory synapses in layer IV outnumber thalamocortical synapses by as much as a factor of 15 (LeVay, 1986; Peters and Payne, 1993; Ahmed et al., 1994). Given these values, the curves shown in Fig. 12-4C seem quite plausible (Stratford et al, 1996). In the case of the narrowest curves, the excitatory and inhibitory curves are so similar as to be difficult to distinguish experimentally. This appears consistent with a recent estimate of cortical orientation currents (Anderson et al., 2000).

Inhibitory Blockade Studies

A direct paradox in the experimental literature on orientation selectivity lies in the dramatic effects observed under different forms of intracortical inhibitory blockade. Extracellular iontophoretic application of the $GABA_A$ antagonist bicuculline methiodide reduced inhibitory synaptic transmission across a local population of cells and disrupted orientation tuning. Sufficiently large bicuculline doses *abolished* orientation selectivity. Bicuculline application also substantially increased response rates. These results argue for a critical role for intracortical inhibition in orientation selectivity (e.g., Sillito et al., 1980). In contrast, our laboratory (Nelson et al., 1994) reported that intracellular blockade of inhibition had negligible effect on orientation tuning (Fig. 12-5A,B). In these experiments whole-cell pipettes were used to deliver CsF-DIDS (4,4′-diisothiocyanostilbene-2,2′-disulfonic acid) solution intracellularly to silence inhibitory voltage conductances (Cl^-, K^+). A mild, fixed hyperpolarizing current was injected to compensate for the increase in spontaneous firing rate. The critical difference between the two sets of inhibitory blockade experiments appears to be the number of cells that lost inhibitory inputs. Disruption of orientation selectivity requires long bicuculline ejection times (Sillito et al., 1980; Nelson, 1991). This suggests that the drug effects spread across a local population of neurons. In contrast, intracellular blockade affects only the recorded neuron. This issue was explored in the model. Bicuculline application was simulated by a 50% reduction in cortical inhibitory synaptic strength for all neurons in the 0° column; synaptic connections onto neurons in other columns were unaffected. CsF-DIDS application was simulated by a 100% reduction in inhibitory synaptic strength (Cl-channels) and an 80% reduction in afterpolarization conductance in a single neuron. The DIDS cell was either

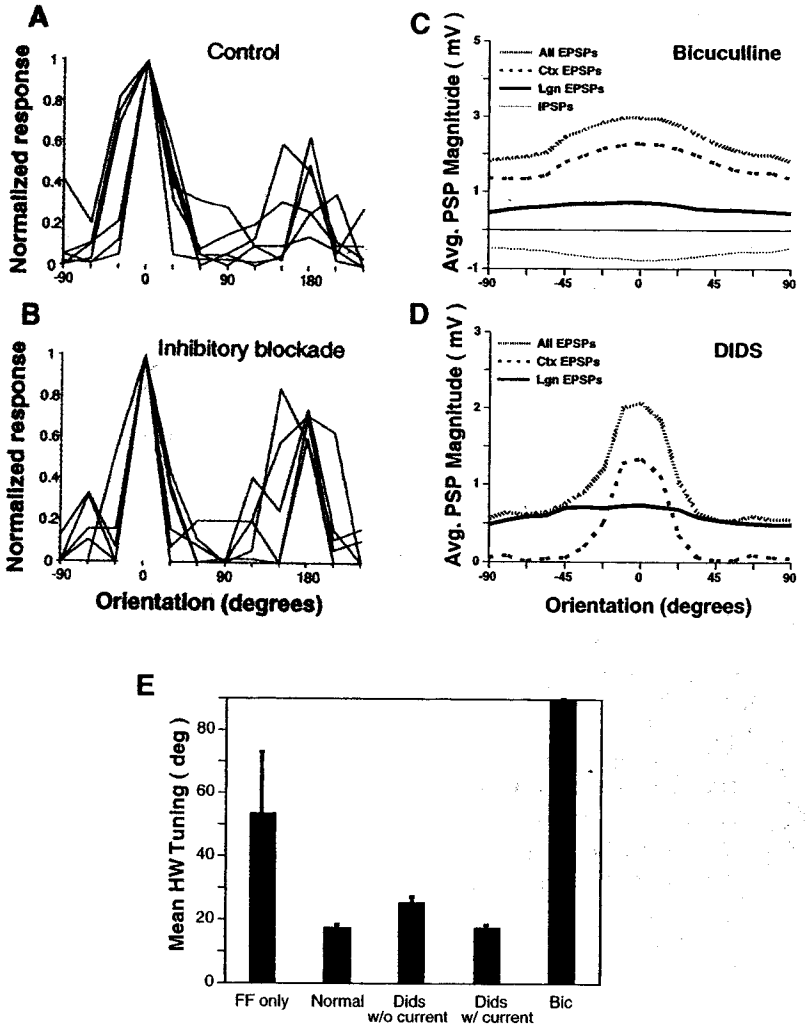

FIGURE 12-5. Inhibitory blockade experiments and model results. (A) and (B): Experimental intracellular blockade of inhibition in single neurons (shown in B) resulted in minimal change in orientation tuning versus normal (shown in A). (C–E) Model results. (C) Simulated bicuculline application reduced inhibition across the column and resulted in a loss of cortical EPSP tuning. Thus bicuculline disrupted both net EPSP tuning and response tuning, despite the fact that strong inhibitory PSPs were still present. In contrast, (D) silencing of inhibition in a single cell had negligible effect on the tuning of other cells. Therefore, cortical EPSPs and net EPSPs retained their orientation selectivity under CsF-DIDS. (E) Summary of model inhibitory blockade results.

injected with a fixed (for all orientations) –0.3 nA hyperpolarizing current or received no injected current.

Under bicuculline application, all cells in the 0° column became unoriented and peak excitatory responses increased by 87% (Fig. 12-5C). Both effects are consistent with experimental reports (Sillito et al., 1980; Nelson, 1991). With inhibitory efficacy reduced, the columnar population amplified responses to all stimuli and thus disrupted tuning. Bicuculline firing rates were higher than the normal firing rates, but they were far below cellular saturation levels (maximum firing rate > 300 sp/s). In agreement with experiment (Sillito et al., 1980; Nelson, 1991), response rates and tuning disruption effects decreased with bicuculline dosage.

DIDS simulations were performed individually for 10 neurons (all excitatory) both with and without injected current. With injected current the 10 cells exhibited mean HW tuning of 17° (Fig. 12-5D), which is identical to the mean tuning of these cells in the normal network. Under DIDS application and without current injection, these 10 cells exhibited mean HW tuning of 25°. Thus the simulations, like experiment, indicate little loss of orientation selectivity with blockade of direct inhibitory inputs. In the model, DIDS cells were sharply orientation selective because they received sharply tuned cortical excitatory input. The iceberg effect caused by the hyperpolarizing current contributed only mildly to the DIDS tuning.

In the model the fundamental difference between the two inhibitory blockade paradigms was the tuning of the intracortical excitatory inputs (Fig. 12-5C,D). Blockade of inhibition in a single cell had a negligible effect on the tuning of other cells in the network. Therefore, the cortical excitatory inputs to the blocked cell retained their sharp orientation tuning and the net input was well tuned (Fig. 12-5D). In contrast, the reduction in inhibition across the local population that occurs with bicuculline dramatically altered the tuning of intracortical excitatory inputs. With insufficient "balancing" inhibition, the recurrent orientation tuning mechanism failed to "emerge" and instead became disruptive. The columnar population amplified responses to all orientations and cortical excitatory cells lost their sharp tuning (Fig. 12-5C).

The inhibitory blockade simulation results are summarized in Fig. 12-5E. Note that bicuculline tuning was substantially worse than the thalamocortical tuning. In comparison, inhibitory models predict that bicuculline tuning should be no worse than the thalamocortical tuning. Thus consideration of intracortical excitation not only provides a mechanism for the persistence of tuning under direct inhibitory blockade of single cells but also provides a more complete explanation than do inhibitory models for the abolition of tuning under extracellular inhibitory blockade.

DISCUSSION

This work demonstrates that recurrent cortical excitatory and inhibitory inputs can rapidly sharpen orientation tuning even in cells that receive unoriented thalamocortical input. The model requires that the orientation column population

receive some thalamocortical bias in orientation that iso-orientation inhibition be somewhat more broadly tuned than iso-orientation excitation, and that cortical excitation and inhibition balance each other. Of these requirements, only the second has proved controversial. How much broader must inhibition be than excitation? Although we initially believed the difference to be substantial, we show here that only a modest difference is required. This appears consistent with recent data (Anderson et al., 2000), although experimental methods with sufficient precision will be required to address this question conclusively.

More potent criticism of this model has come in the form of experimental evidence that has resurrected the linear feedforward model of Hubel and Wiesel. Efforts to silence cortical inputs have revealed little change in the sustained component of orientation tuning of many layer IV cells (Ferster et al., 1996; Chung and Ferster, 1998). These experiments demonstrate clearly that feedforward inputs play a significant role in orientation tuning, but also raise other issues. Intracellular records in the cortical silencing experiments (Ferster et al., 1996; Chung and Ferster, 1998) reveal tuning that appears to be substantially broader than that observed in normal extracellular recordings. Intracellular recordings also appear not to reveal the constant DC component across orientation that is predicted by the Hubel-Wiesel model (Carandini and Ferster, 2000). Although careful mapping of thalamic inputs to simple cell subfields has reported a close spatial correlation (Reid and Alonso, 1995) (see Chapter 8), it has not revealed the high aspect ratio of subfields that the linear model requires. A recent study (Gardner et al., 1999) reported that the linear component only accounts for about half of orientation tuning; the rest is nonlinear. In addition, several different groups have reported that orientation tuning rapidly sharpens at the beginning of responses (Ringach et al., 1997; Shoham et al., 1999; Dragoi et al., 1999), which is a key prediction of our model.

Shunting inhibition is another potential mechanism that has been revealed by recent experiments (Borg-Graham et al, 1998; Hirsch et al., 1998). Although the shunting appears far too brief to support the central hypothesis of normalization models (Heeger, 1992; Carandini and Heeger, 1994), the strength and timing of the shunting suggest that it may play a powerful role in shaping cortical responses. One potential utility is in controlling the strength of recurrent excitatory inputs. The implications of this use are just starting to be addressed (Chance and Abbott, 2000). At this time, it appears likely that orientation selectivity will not be accounted for by a single mechanism, but rather by a combination of feedforward, cortical inhibitory, cortical excitatory, and spike threshold mechanisms. A newer model (Troyer et al., 1998) invokes recurrent excitation between neurons to amplify phase-selective responses and strong inhibition from spatially opponent subfields to generate contrast invariance in orientation selectivity. However, key assumptions of the model, such as a population of neurons that respond in contrast-dependent manner to all orientations, remain untested. Other evidence suggests that feedback from cortex to thalamus (Murphy et al., 1999) and cellular adaptations may also contribute (Anderson et al., 2000b). All of this suggests that

this particular cortical computation is far more complex than the field had anticipated. At the same time, orientation tuning is fundamentally a nonlinear property of V1 neurons, and it appears parsimonious to invoke nonlinear mechanisms to explain its major nonlinear features.

EFFECT OF LONG-RANGE CONNECTIONS ON ORIENTATION-SPECIFIC RESPONSES

INTRODUCTION

In this section, we present modeling (Somers et al., 1998) and experimental results (Toth et al., 1996) on dynamic local and long-range receptive field effects. We present a recurrent cortical model suggesting how the net effect on a cell, of stimulating one portion of the receptive field, can switch between excitatory and inhibitory in different stimulus contexts, without requiring dynamic cellular or synaptic properties. We also present experimental results supporting this notion. This model extends the model from the prior section by incorporating long-range (> 1.5 mm) intracortical excitatory connections (Rockland and Lund, 1982; Gilbert and Wiesel, 1983) (see Chapters 10 and 11).

The dynamic response modeling ideas arose out of consideration of cortical gain control issues (Somers et al., 1995b). To ensure the stability of a recurrent excitatory network, inhibition must be relatively strong at high drive levels (to prevent run-away positive feedback); yet, inhibition cannot be allowed to be too strong at low, suprathreshold drive levels (or else responses will be squashed). These same gain control principles can also produce dynamic receptive field effects with fixed circuitry. It turns out that this computational idea has interesting pieces of data to support it, including three previously unconnected phenomena: supersaturation, contrast-dependent length summation, and surround facilitation and suppression. In all three examples, receptive field regions shift from having excitatory influences to inhibitory influences as the contrast (and hence not excitatory drive) increases for the classical receptive field component of the stimulus.

Increasing the contrast of a stimulus in the receptive field can, at high contrast, actually cause responses of many V1 cells to decline or "supersaturate" (Li and Creutzfeldt, 1984) (Fig. 12-6A). This effect has been observed at contrast levels for which LGN responses have not saturated or supersaturated (Albrecht and Hamilton, 1982; Bonds 1991). A related phenomenon concerns the receptive field length of end-stopped cells. These cells typically respond maximally to high contrast stimulus bars of a certain length (and orientation), and responses decline for longer bars (e.g., Hubel and Wiesel, 1965), presumably owing to encroachment of the stimulus on inhibitory zones located at the ends of excitatory regions. End zones have maximal inhibitory effect when activated by stimuli of the preferred orientation (Orban et al., 1979; DeAngelis et al., 1994). However, these inhibitory zones can become excitatory as stimulus contrast is decreased, so that low contrast (preferred orientation) bars have longer optimal lengths than do high contrast

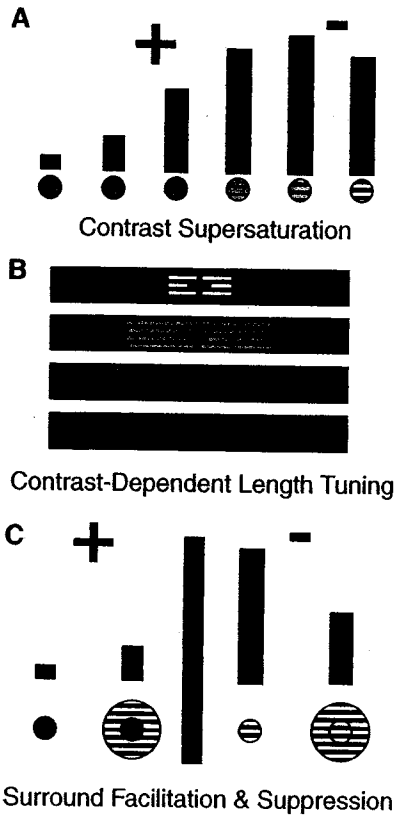

FIGURE 12-6. Schematic representation of different receptive field influences that shift from excitatory to inhibitory as central stimulus contrast increases. **(A)** A high-contrast surround stimulus facilitates the response of a low-contrast center stimulus, but the same surround-stimulus suppresses responses when the center stimulus is of high contrast. **(B)** Increasing the contrast of a center stimulus alone can decrease responses at very high contrast levels ("contrast supersaturation"). This suggests that the excitatory portion of the classical RF can become inhibitory. **(C)** Decreasing the contrast of a stimulus can cause the region of end-stopping to shift outward over the receptive field. At low contrasts, length summation can extend several degrees into the "inhibitory end-zones." Thus, the border between excitatory and inhibitory regions appears to shift with stimulus contrast. For all three receptive field effects, modulatory stimuli tend to have both the strongest facilitatory and strongest suppressive effects when oriented at the preferred orientation of the classical receptive field.

bars (Fig. 12-6B). This effect was first reported briefly (Jagadeesh and Ferster, 1990; Jagadeesh, 1993) but has since been replicated (Sceniak et al., 1999). A stimulus placed outside the classical receptive field can sometimes enhance responses (Maffei and Fiorentini, 1976; Knierim and Van Essen, 1992) and sometimes suppress responses (Blakemore and Tobin 1972; Nelson and Frost, 1978; Gulyas et al., 1987; Born and Tootell, 1991; Knierim and Van Essen, 1992;

Grinvald et al., 1994) (Fig. 12-6C). However, this seeming paradox had not been fully explored. In response to the model results, our laboratory performed a number of studies to investigate this dynamic behavior (Toth et al., 1996). Work by others has also supported and expanded this notion (Levitt and Lund, 1997; Sengpiel et al., 1997, 1998; Polat et al., 1998).

This work suggests that the relevant unit of receptive field integration is not the single neuron, but rather the local population of cells within a column of 300 to 500 μm diameter. In the single unit view, a fixed input to a fixed circuit will always exert a fixed influence on responses (Hartline, 1940; Kuffler, 1953; Movshon et al., 1978; Jones and Palmer, 1987; DeAngelis et al., 1995); however, in the population view, the net influence of a fixed input can change, provided that the integrating population consists of inhibitory and excitatory subpopulations with different (static) response properties.

KEY ASSUMPTIONS OF THE MODEL

The dynamic receptive field effects demonstrated here rely on an asymmetry between excitatory and inhibitory inputs in the local cortical circuitry. The critical property is that net inhibitory local circuit influences grow stronger at a greater rate than that of local excitatory influences as external drive levels increase. This idea is also supported by electrical stimulation experiments in slices of visual cortex (Hirsch 1995; Weliky et al., 1995). We (Somers et al., 1998) have proposed two specific nonlinear mechanisms for achieving this local circuit asymmetry; however, other plausible circuit nonlinearities could achieve the same functional results. The first (which we review here) is to utilize inhibitory neurons that, as a population, have higher response gain and higher contrast threshold than excitatory neurons. Based on intracellular data (McCormick et al., 1985), it is known that fast-spiking or inhibitory cells have much higher response gains than regular-spiking or excitatory neurons. However, the requirement for a higher contrast threshold has not been examined experimentally, and this assumption represents one experimental prediction of our model. Because this threshold difference need occur only at a population level, it is possible to achieve this result if multiple classes of inhibitory neurons, some with high thresholds and some with low thresholds (or a continuum) exist. Lund and colleagues (c.f., Lund et al., 1995) have identified several morphological classes of inhibitory neurons in V1 (see Chapter 1). Our analysis suggests that high threshold inhibitory neurons play a central role in gain control.

Synaptic physiology studies (Abbott et al., 1997; Tsodyks and Markram, 1997) indicate that rapid activity-dependent changes in synaptic efficacy at excitatory-excitatory cortical synapses may profoundly influence cortical processing. We suggest that if efficacy changes at excitatory-inhibitory synapses have the opposite sign, as is suggested by the data of Thomson and Deuchars (1994), then modulation of short-range synapses is sufficient to support contextual switching effects for both local and long-range inputs to the local cortical circuitry. Because this circuit with short-term synaptic plasticity cannot be called "fixed," we have

omitted the result in this chapter and refer the interested reader to Somers et al. (1998). The important point is that the central requirements of the model can be achieved by diverse local circuit mechanisms.

MODEL STRUCTURE AND IMPLEMENTATION

The model (Somers et al., 1998) extends our prior local circuit model of orientation selectivity (Somers et al., 1995a) by incorporating long-range intracortical excitatory connections. Cortical circuitry under a 3.5 mm × 7 mm patch of primary visual cortex was represented by a model with 20,250 spiking cortical neurons and more than 1.3 million cortical synapses. Whenever possible, known anatomical values, ratios, and constraints were imposed on the model. In scaling up such a nonlinear system, parameter modifications were unavoidable; however, the essential behaviors of the earlier model (i.e., orientation sharpening, and amplification) persist in the present model. Neurons were organized into a 45 × 90 grid of "mini-columns" (Peters and Yilmaz, 1993) based on an orientation map obtained by optical recording of intrinsic signals of cat visual cortex (Toth et al., 1996) (Fig. 12-7).

Both excitatory and inhibitory neurons made short-range intracortical connections, whereas only excitatory neurons made long-range connections (see Chapter 10). Each type of connection targeted both excitatory and inhibitory postsynaptic neurons (Beaulieu and Somogyi, 1990; McGuire et al., 1991; Anderson et al., 1994). Short-range connection probabilities fell linearly with distance. Long-range excitatory neurons preferentially targeted neurons with orientation preferences similar to their own (Gilbert and Wiesel, 1989; McGuire et al., 1991; Malach et al., 1993). Connection probabilities declined linearly with the orientation difference between presynaptic and postsynaptic cells, from $\rho_{peak} = 0.005$ at $\varphi=0°$ to $\rho_{edge}=0.001$ at $\varphi=90°$.

We used two differences between the two cell classes as one way to create an asymmetry in the local circuitry that provides a local gain control mechanism. Fast-spiking (FS) or inhibitory neurons have higher input resistances and thus have higher current gains (greater slope of the frequency versus current plot) than those of regular striking (RS) or excitatory neurons (McCormick et al., 1985). Current thresholds for FS and RS neurons are similar, but inhibitory neurons receive substantially fewer synapses and presumably less synaptic current than excitatory neurons. Thus, we hypothesize that FS neurons have higher functional thresholds (e.g., contrast thresholds) than RS neurons. The combination of higher gain and threshold for a population of inhibitory neurons is one mechanism used to achieve a generalized gain control mechanism in the local circuitry. The essential nonlinearity here is that the ratio of local excitatory currents to local inhibitory currents evoked by a stimulus configuration should be high for low stimulus intensities and should decrease at higher stimulus intensities.

Stimuli consisted of circular ("center") and annular ("surround") gratings of differing contrasts, orientations, and radii. Central RF studies used only a central grat-

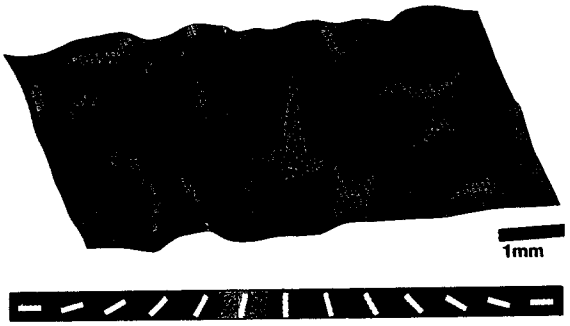

FIGURE 12-7. Connectivity of cortical circuitry in the model. The color map represents the orientation preference of each cortical mini column. The pattern of intracortical connections to cells in the central (Yellow) mini-column is represented by the surface amplitude, which codes the net (Σ Excit – Σ Inhib) strength of intracortical connections from each column to the cells of the central column. Three classes of intracortical connections are included in the model: short-range excitatory, short-range inhibitory, and long-range excitatory. Short-range connections are densest in the vicinity of the presynaptic cells and fall off with distance. Short-range excitatory connections are more numerous, but more spatially restricted than short-range inhibitory connections. Long-range excitatory connections can span the entire circuit and preferentially target cells with similar orientation biases. All connections target both excitatory and inhibitory neurons. See color insert for color reproduction of this figure.

ing with a diameter approximately equal to the RF (1°). End-stopping studies varied this diameter. Surround studies combined a 1° diameter center stimulus with a surround annulus (1° inner diameter; 4° outer diameter). Thalamic neuron responses to these stimuli increased linearly with log contrast. LGN responses were independent of stimulus orientation, phase, and spatial frequency. Converging thalamocortical inputs to a column were biased for a particular stimulus orientation and location (Hubel and Wiesel, 1962), and orientation selectivity was enhanced by intracortical connections (Somers et al., 1995a). The average firing rate of the converging thalamocortical input to single cortical neurons was a function of stimulus orientation (θ_{cent}, θ_{surr}), contrast (%$Cont_{cent}$, %$Cont_{surr}$), size, and position.

MODEL PERFORMANCE

Contrast Saturation and Supersaturation

The model captures physiological responses to oriented grating stimuli of differing contrasts presented within the classical receptive field. Model behavior is analyzed for a population of neurons lying in the central orientation domain of the model (yellow peak of Fig. 12-7). Figure 12-8A shows mean responses of excitatory cortical neurons to oriented grating stimuli of different contrasts presented within the classical receptive field. Responses were averaged for the same set of neurons in 20 networks, each constructed with the same connectivity probability rules.

To isolate cortical effects, thalamic responses were designed to increase linearly with log contrast. The dotted lines in Fig. 12-8A show contrast response curves for the cortical neurons at two different stimulus orientations when intracortical synapses are shut off and only thalamocortical inputs are active; note the linear responses above threshold. In the full model, with intracortical synapses active, cortical responses (data points and solid lines in Fig. 12-8A) exhibit a saturation nonlinearity at higher contrasts. This occurs at contrast levels for which thalamic responses have not yet saturated. Contrast saturation in the model is achieved as a network property rather than as a cellular property. Saturation response levels vary with stimulus orientation. Consistent with our prior model (Somers et al., 1995a), cortical inputs sharpen orientation tuning (compare differences between 0° and 20° responses). Note that intracortical connections amplify responses to low contrast stimuli at the preferred orientation, but attenuate responses to high contrast stimuli. Contrast saturation in our model reflects a gain change in local cortical circuitry that results from an asymmetry between the properties of excitatory and inhibitory neurons. Inputs from inhibitory neurons grow proportionally stronger at high levels of input drive; population responses for inhibitory neurons saturate only when LGN responses saturate.

For a subpopulation of modeled neurons (18 of 36 cells), a decline in response at high contrast was observed (Fig. 12-8B). Li and Creutzfeldt (1984) described this behavior in detail, calling the decline "supersaturation," because it occurs at contrast levels beyond which normal contrast saturation can be observed. Those authors suggested that supersaturation might result from reduced drive from thalamic sources at high contrasts; here, we show that a purely cortical mechanism is sufficient. The supersaturation effect, although infrequently discussed, can also be seen in other experimental reports (Albrecht and Hamilton, 1982; Bonds, 1991). Thus, for many cells, even the classical excitatory receptive field can have inhibitory effects when stimulation is strong.

Length-tuning

The effects of varying stimulus length and contrast were also systematically explored within the simulations. Responses to a high contrast visual stimulus were observed to decline beyond a characteristic preferred size (see top curve of Fig. 12-8C). Thus the model exhibited a form of length tuning or end-stopping (Hubel and Wiesel, 1965). Consistent with experiments (Orban et al., 1979; DeAngelis et al., 1994), high contrast iso-orientation stimuli that extend into end-zone (or side band) regions have potent inhibitory effects on responses to the central stimulus. In agreement with experimental findings (Jagadeesh and Ferster, 1990; Jagadeesh 1993; Sceniak et al., 1999), the length of the excitatory receptive field increased with decreasing contrast, and at low-stimulus contrasts responses to optimal orientation gratings continued to increase monotonically. Both the experiment and simulations indicate that the borders between excitatory and inhibitory regions shift depending on the level of stimulus contrast.

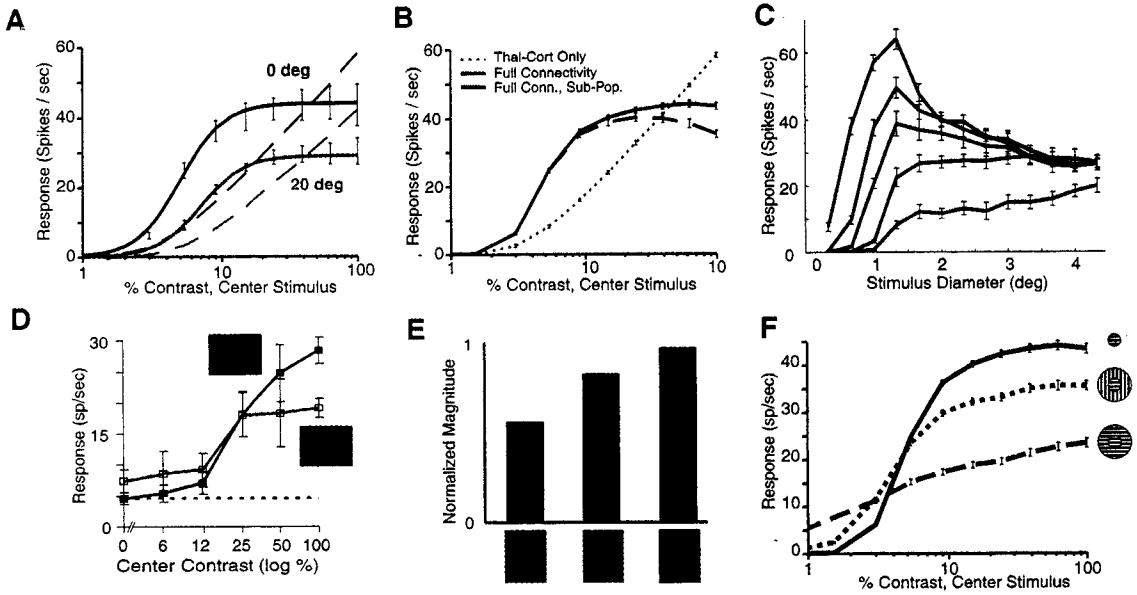
A
Response (Spikes / sec)
0 deg
20 deg
% Contrast, Center Stimulus
B
Thal-Cort Only
Full Connectivity
Full Conn., Sub-Pop.
Response (Spikes / sec)
% Contrast, Center Stimulus
C
Response (Spikes / sec)
Stimulus Diameter (deg)
D
Response (sp/sec)
Center Contrast (log %)
E
Normalized Magnitude
F
Response (sp/sec)
% Contrast, Center Stimulus

Facilitation Suppression

While preserving classical receptive field properties, the model also captures paradoxical extraclassical receptive field modulations (Knierim and Van Essen, 1992; Toth et al., 1996; Levitt and Lund, 1997; Sengpiel et al., 1997, 1998; Polat et al., 1998; Sillito et al., 1995). The contrast of a central grating was varied under three different surround stimulus conditions: no surround, a high contrast cross-orientation surround stimulus, and a high contrast iso-orientation surround stimulus. The modulatory influence of "surround" gratings on responses to optimal orientation "center" stimuli shifts from facilitatory to suppressive as center stimulus contrast increases (Fig. 12-8F). Compare this with experimental results from our laboratory (Toth et al., 1996) using single unit recording (Fig. 12-8D) and optical recording (Fig. 12-8E) techniques; a clear switch in receptive field influence is seen in both the data and in the model. Model simulations also obtain the result that both facilitation and suppression effects are strongest for iso-orientation surround stimuli (Knierim and Van Essen, 1992; Toth et al., 1996; Weliky et al., 1995; Sillito et al., 1995; Levitt and Lund, 1997). These effects emerge from the local intracortical interactions (as shown later) and do not require synaptic plasticity (cf. Hirsch and Gilbert, 1991; Gilbert et al., 1996) or complex cellular properties (cf., Bush and Sejnowski, 1994). This model also provides the first unified account of these classical and extraclassical RF modulations.

FIGURE 12-8. Model and experimental results on shifting excitatory and inhibitory regions of the receptive field. **(A)** Contrast response functions of model. Grating stimuli were shown at the preferred orientation (black curves) and 20° off of preferred (gray curves). Response of the full model circuit is shown with solid curves; response to thalamocortical inputs alone is shown with dashed lines. Cortical inputs strongly amplify responses to low suprathreshold contrasts, but attenuate responses to high contrasts. Cortical inputs also sharpen orientation selectivity. **(B)** For a subpopulation (18 of 36) of these neurons (dashed line), responses decline at high contrasts (supersaturation). **(C)** Response versus stimulus diameter at five different contrast levels (60%, 10%, 5%, 3%, and 2%) of the preferred orientation (10 trials, SD shown). For the highest contrast stimuli (top curve) responses are maximal for small stimuli (< 1.5°) and decrease for larger stimuli. As stimulus contrast decreases (lower curves), excitatory length summation occurs for progressively larger stimuli. Experimental results on surround facilitation and suppression from **(D)** single unit recordings and **(E)** optical recording of intrinsic signal. Central-grating stimuli were presented alone and again in conjunction with a high-contrast iso-orientation surround grating. Only the contrast of the central grating was changed. Resulting contrast response functions (CRFs) for the composite stimulus were higher at low center contrasts and lower at high center contrasts than center-only CRFs. Suppression and facilitation effects were largely unaffected by phase relation between center and surround stimuli. Optical recording data **(E)** show same effects, using only end points of CRFs. **(F)** Model results on facilitation and suppression produced by high-contrast surround stimuli. Responses of the same model neurons to varying contrast levels of a center stimulus under three fixed surround conditions: no surround (solid), high contrast cross-orientation surround (dotted), and high-contrast iso-orientation surround (dashed). Both surround stimuli increase responses to low-contrast centers but decrease responses to high-contrast center stimuli. Both facilitation and suppression effects are stronger for the iso-orientation surround.

Here, we have demonstrated one mechanism to produce the local circuit asymmetry: a population-level bias among inhibitory neurons to have higher gain and higher contrast thresholds than excitatory cells. Elsewhere we (Somers et al., 1998) have demonstrated a second mechanism: differential adaptation and enhancement at local intracortical excitatory synapses onto excitatory and inhibitory neurons, respectively (Thomson et al., 1993a, 1993b, 1995; Thomson and West, 1993; Thomson and Deuchars, 1994).

DISCUSSION

The functional asymmetry in the local cortical circuitry provides a generalized contrast gain control mechanism that can be accessed by all input sources. At low center-driving contrasts, local cortical excitation provides strong amplification of suprathreshold inputs. As center drive levels increase, local inhibition grows to reduce the cortical amplification factor. As a result, the model achieves saturating and supersaturating contrast response functions as a local circuit property. This result is consistent with experimental evidence that contrast saturation occurs when neither cellular firing rates nor synaptic inputs have reached plateau values. Thus, we suggest that the notion that excitation saturates is incorrect; rather, inhibition counterbalances excitation. The model makes the specific prediction that cortical amplification is strongest for low-contrast, suprathreshold stimuli (of the preferred orientation) and that amplification decreases and may even become attenuation as contrast increases.

This local circuit form of gain control, unlike cellular or input saturation ideas, also captures spatial contrast gain effects. Excitatory receptive field regions are spatially restricted when the total inputs are strong, but enlarge, as inputs become weaker. These expansion-contraction effects are adaptive in that they collect (excitatory) information more widely when the overall signal is weak but restrict their spatial spread when the signal from more central receptive field regions is stronger. It should be noted that the term *contrast gain control* has an ambiguous meaning in the literature, referring both to instantaneous contrast saturation as discussed here and slower acting contrast adaptation.

Sceniak et al. (1999) performed a linear, difference-of-gaussians analysis of their contrast-dependent dependent length summation data and found that their effects were best fit by allowing the excitatory space constant to shrink as stimulus contrast increased. This linear analysis suggested that surround strength effects were variable, increasing for some cells and decreasing for others. On this basis, these authors have criticized our long-range model because it suggests that excitatory and inhibitory changes are coupled; however, this analysis is problematic. Our model makes a nonlinear prediction about the excitatory and inhibitory strength parameters; this was not tested in their analysis. It would be interesting to see this prediction analyzed with their data. One might argue that a linear interpretation is simpler than a nonlinear one; however, in this case, the linear model *requires* that the functional connectivity of excitatory connections change with

stimulus contrast, whereas the nonlinear model requires no such changes. One mechanism that they suggest for functional connectivity changes is synaptic depression at excitatory synapses, which is the second mechanism that we proposed and demonstrated (Somers et al., 1998).

Co-aligned, iso-orientation surround stimuli tend to facilitate responses for both high and low-contrast center stimuli (Kapadia et al., 1995; Polat et al., 1998). This effect may be related to perceptual contour integration (Grossberg and Mingolla, 1985; Field et al., 1993; Polat and Sagi, 1993) and may result from excitatory-excitatory connections between co-aligned, iso-orientation cell clusters (Bosking et al., 1997). Long-range connections in our model are not biased for spatial anisotropies. Our model could achieve alignment-specific facilitation by adding aligned long-range inputs that are more biased to synapse onto excitatory targets than are the present alignment nonspecific long-range inputs. Our model could similarly be extended to incorporate other specific patterns of long-range excitation, such as feedback from area V2 (Bullier et al., 1996).

SUPRAOPTIMAL RESPONSES AND DYNAMIC PROPERTIES OF RECURRENT INHIBITION

INTRODUCTION

We have described in the previous section how a functional asymmetry in the local cortical circuitry provides a sufficient explanation for the contrast dependency of contextual interactions. When the classical receptive field is optimally stimulated at high contrast, the presence of an iso-oriented surround stimulus increases the local inhibitory input to reduce the cortical gain, whereas when the center drive decreases, the local excitation provides strong amplification of suprathreshold inputs. However, it is unlikely that this mechanism would be able to explain cross-orientation surround facilitation (i.e., the fact that stimulating the surround with a grating whose orientation differs significantly from the cell's preferred orientation facilitates responses to optimal stimulation within the center) (Sillito et al., 1995; Levitt and Lund, 1997). In this case neurons respond beyond the level expected after stimulation with the optimal orientation (Fig. 12-9A). One prediction of our long-range model (Somers et al., 1998; also Stemmler et al., 1995) is that a cross-oriented surround would provide weak input to the local populations of excitatory and inhibitory neurons such that cortical responses are maintained around center-alone response levels.

To explore potential mechanisms that would explain the emergence of supraoptimal responses elicited by the cross-oriented surround, we reasoned that at high-contrast center and surround stimulation local inhibitory populations receive tonic inputs that show orientation specificity. Indeed, it has been reported (Weliky et al., 1995; Weliky and Katz, 1994) that activation of long-range horizontal connections evokes direct iso-orientation excitatory and multisynaptic

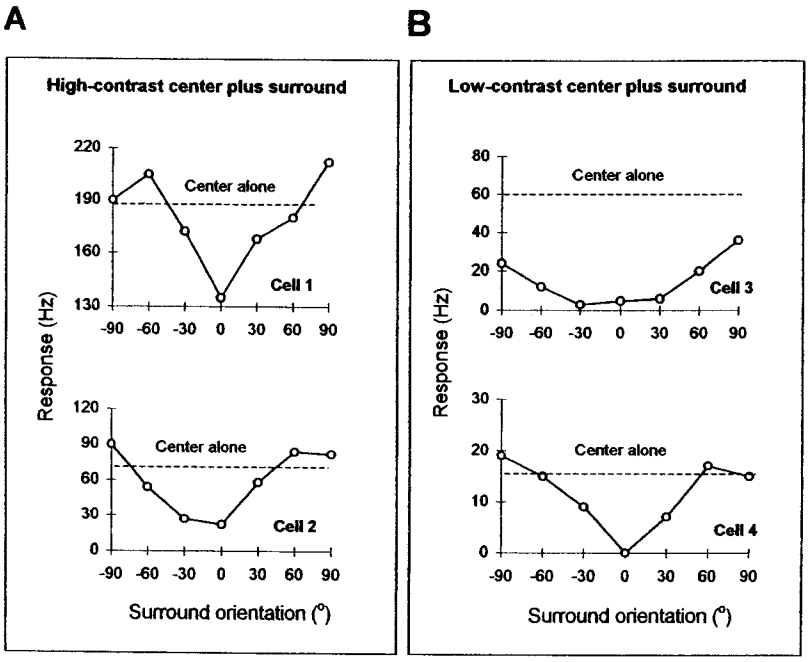

FIGURE 12-9. Contrast and orientation dependence of contextual effects (experimental data). (A) Experimental data: Responses to the high-contrast optimal center stimulus paired with high-contrast surround gratings of varying orientations. Cells 1 and 2 are adapted from Fig. 12-1 (cells A and D) of Levitt and Lund (1997). (B) Experimental data: Responses to the low-contrast optimal center stimulus paired with high-contrast surround gratings of varying orientations. Cells 3 and 4 are adapted from Fig. 12-1 (cells D and E) of Levitt and Lund (1997). Dashed lines in all panels indicate response to the optimal stimulus alone.

inhibitory responses from local pyramidal cells such that there is stronger activation of iso-orientation domains and gradually weaker activation of cross-orientation domains (see Chapters 10 and 11). It is thus possible that for certain center-surround orientation configurations, the stronger activation of selected local inhibitory neurons could trigger disinhibitory mechanisms that would facilitate responses in the presence of a cross-oriented surround. Disinhibitory interactions have a well-established role in other brain systems (e.g., Ito et al., 1968; Kelly and Renaud, 1974; Getting and Dekin, 1985; Hultborn et al., 1971), and yet the function of disinhibitory mechanisms in the visual cortex has not been explored. In this section we describe how recurrent inhibition in V1 can trigger disinhibitory interactions that help explain cross-orientation surround facilitation. Previous theoretical considerations, (Blomfield, 1974; Koch and Poggio, 1985) have suggested that inhibition could play a crucial vetoing role in the emergence and shaping of receptive field properties, such as direction (and possibly orientation)

selectivity. However, these models have considered the properties of inhibitory projections to excitatory neurons without exploring the functional role of recurrent inhibition.

MODEL STRUCTURE AND IMPLEMENTATION

We have used a model of recurrent inhibition (Dragoi and Sur, 2000) to understand why surround stimuli presented at nonoptimal orientations drive neurons beyond optimal responses (obtained by high-contrast center stimulation at the preferred orientation), whereas when the CRF is stimulated at low contrast, the facilitatory effects disappear (Sillito et al., 1995; Levitt and Lund, 1997) (Fig. 12-9). The model incorporates short-and long-range interactions that describe the processing of information at two sequential stages: LGN and V1. The model configures 8,712 LGN neurons arranged on the array of 11 × 11 locations, with 72 cells per each location of the visual patch and 17,424 cortical neurons.

Cellular Models

LGN cells are modeled as single units whose mean rate of firing is given by:

$$dLGN_i/dt = -0.01\ LGN_i + R_i\ (1 - LGN_i)$$

where LGN_i represents the lateral geniculate cell. The retinal input, R_i, is set such that thalamic responses increase linearly with the log of stimulus contrast. R_i is maximal when the preferred orientation of the cortical cell that corresponds topographically to LGN_i matches the stimulus orientation, and it decays exponentially to zero with increasing orientation differences (Dragoi and Sur, 2000). The spread of geniculate inputs to the cortex ensures that each LGN cell synapses on a group of cortical cells with a broad range of orientations (with a spread of 60°). Cortical cells receive center stimulation as an oriented input stimulus applied to the receptive field center of LGN cells and surround stimulation as oriented stimuli applied to the surrounding hypercolumns.

Excitatory and inhibitory cortical neurons are modeled separately as single units whose mean rate of firing is given by:

Excitatory cells

$$dE_i/dt = -0.01\ E_i + (J^{fe}\ F_i + \Sigma_j\ J_{ij}^{ee}\ E_j + \Sigma_j\ J_{ij}^{me}\ E_j)\ (1 - E_i) - \Sigma_j\ J_{ij}^{ie}\ I_j\ E_i$$

Inhibitory cells

$$dI_i/dt = -0.01\ I_i + r\ (J^{fi}\ F_i + \Sigma_j\ J_{ij}^{ei}\ E_j + \Sigma_j\ J_{ij}^{mi}\ E_j)\ (1 - I_i) - \Sigma_j\ J_{ij}^{ii}\ I_j\ I_i$$

where E_i represents excitatory and I_i represents inhibitory cells. In agreement with experimental evidence (Connors et al., 1982; McCormick et al., 1985), model inhibitory cells have a higher firing rate than excitatory cells ($r = 3$). Each cortical cell receives stimulus-specific feedforward input, F_i, as the summed response of LGN cells centered at i with a spread of 60°. J^{fe} and J^{fi} are the

strengths of feedforward connections and are equal for excitatory (fe) and inhibitory (fi) cells. J_{ij}^{ee} and J_{ij}^{ei} are the strengths of recurrent excitatory connections (ee) and excitatory projections to inhibitory cells (ei). J_{ij}^{ie} and J_{ij}^{ii} are the strengths of the inhibitory projections to excitatory cells (ie) and inhibitory cells (ii). J_{ij}^{me} and J_{ij}^{mi} are the strengths of long-range (modulatory) inputs to excitatory cells (me) and inhibitory cells (mi).

Short-range Intracortical Connections

Excitatory neurons are interconnected by recurrent excitatory synapses (Martin, 1988; Peters and Payne, 1993), whereas inhibitory neurons are interconnected by recurrent inhibitory synapses (Beaulieu and Somogyi, 1990; Kisvarday et al., 1993; Sik et al., 1995). In addition, local excitatory cells excite neighboring inhibitory cells, which in turn inhibit excitatory cells (Beaulieu and Somogyi, 1990; McGuire et al., 1991; Anderson et al., 1994a) (Fig. 12-10A). Short-range excitatory and inhibitory connection strengths decrease as cortical neurons become more widely separated in orientation (Fries et al., 1977; Nelson and Frost 1978; Miller, 1992). The strength of excitatory connections decays exponentially from 0.01 at distance zero to 75% of the peak value at 40° orientation difference between presynaptic and postsynaptic cells; the strength is 0 beyond 40°. Consistent with evidence from cross-correlation studies (Toyama et al. 1981; Michalski et al., 1983; Hata et al., 1988) and from combined imaging and intracellular recording (Tucker and Katz, 1998), intracortical inhibitory connections arise from cells with a broader distribution of orientation preferences than do intracortical excitatory connections. However, given the current disagreement on the exact orientation spread of inhibitory connections (Ferster, 1988; Hirsch and Gilbert, 1991; Tucker and Katz, 1998; Roerig and Katz, 1998), we have restricted inhibitory inputs to an orientation difference of 60° between presynaptic and postsynaptic cells. Inhibitory connection strengths are stronger than excitatory connections (Komatsu et al., 1988; Thomson and West, 1993; Thomson and Deuchars, 1994), and they decay exponentially with distance from a maximum value at distance 0 to 10% of the peak value at 60° orientation difference between presynaptic and postsynaptic cells. The strength of inhibitory connections is 0 beyond 60°.

Long-range Intracortical Connections

Long-range horizontal connections (Gilbert and Wiesel, 1979; Rockland and Lund, 1982a; Livingston and Hubel, 1984; Martin and Whitteridge, 1984) link cells across distinct regions of the visual field and spread across four orientation hypercolumns (or locations) in the model. Model long-range horizontal connections are excitatory and originate from pyramidal cells in the surround (cf. Gilbert and Wiesel, 1989) (Fig. 12-10A). These cells contact other pyramidal cells, as well as nearby inhibitory cells that are locally interconnected within a range of ± 60° (Kisvarday et al., 1986; McGuire et al., 1991). Model activation of horizontal connections evokes direct iso-orientation excitatory and multisynaptic inhibitory

responses from local pyramidal cells in an orientation-dependent fashion: stronger activation of iso-orientation domains and gradually weaker activation of cross-orientation domains. We set the strengths of model long-range horizontal connections as being maximal when they connect cortical cells with the same orientation preference; the strengths gradually decrease with increasing relative orientation between cells (Weliky et al., 1995; Weliky and Katz, 1994). Long-range connection strengths decay exponentially from $J_i^{mi} = 0.03$ and $J_i^{me} = 0.01$ at distance 0 to 25% of the peak value at 60° orientation difference between presynaptic and postsynaptic cells.

MODEL PERFORMANCE

Analysis of Recurrent Inhibition

Our goal in the simulations is to understand how neuronal responses are modulated by changes in the balance between local excitation and inhibition as a result of surround stimulation. Therefore, the receptive field center was always stimulated at the optimal orientation, whereas surround orientation was varied systematically from 0° to 180° to fully investigate the orientation dependence of contextual effects. Figure 12-10B–E shows the changes in excitatory and inhibitory cortical responses in a representative population of cells with orientation preferences in the range [–30°, 75°]. The high-contrast surround stimulus is oriented either at 0° (maximum suppression) or 60° (maximum facilitation), whereas the orientation of the center stimulus is fixed at 0°. In all the simulations the center stimulus is either presented at 100% (high) or 15% (low) contrast level.

High-contrast Center Stimulation

When the surround is oriented at 60°, strongly it activates the inhibitory cells in the vicinity of iso-orientation domains (e.g., 60°) and more weakly the inhibitory cells in the vicinity of non-iso-orientation domains (e.g., 0°) (Fig. 12-10A). The surround modulation is orientation-dependent: pyramidal cells outside the CRF project more strongly to iso-orientation domains and only weakly to non-iso-orientation domains (e.g., the projection to the horizontal pyramidal cell in Fig. 12-10A) and to the neighboring inhibitory cells. Figure 12-10B–E represents the changes in inhibitory and excitatory responses relative to the center alone condition. Because of their higher firing rates, inhibitory cells with orientation preference close to that of the surround (i.e., the cells with orientation preferences near 60°) are able to fire continuously in response to the tonic center and surround stimuli and thus exert tonic inhibition on their postsynaptic targets (i.e., inhibitory and excitatory cells with orientation preferences near 0°). The effect of this interaction can be seen in Fig. 12-10B, which shows that the activity of inhibitory cells oriented away from the surround orientation (e.g., the 0° cells) diminishes below the center alone condition. The net effect of this removal of tonic inhibition, or disinhibition, from pyramidal cells in the vicinity of the 0°

domain is an increase in the strength of excitation relative to the center-alone condition (Fig. 12-10C). This explains the supraoptimal responses obtained when the surround is cross-oriented with respect to the center stimulus (Fig. 12-11A). However, when the surround is oriented at 0°, there is an increase in the inhibitory responses above the center-alone condition (Fig. 12-10B) that decreases the

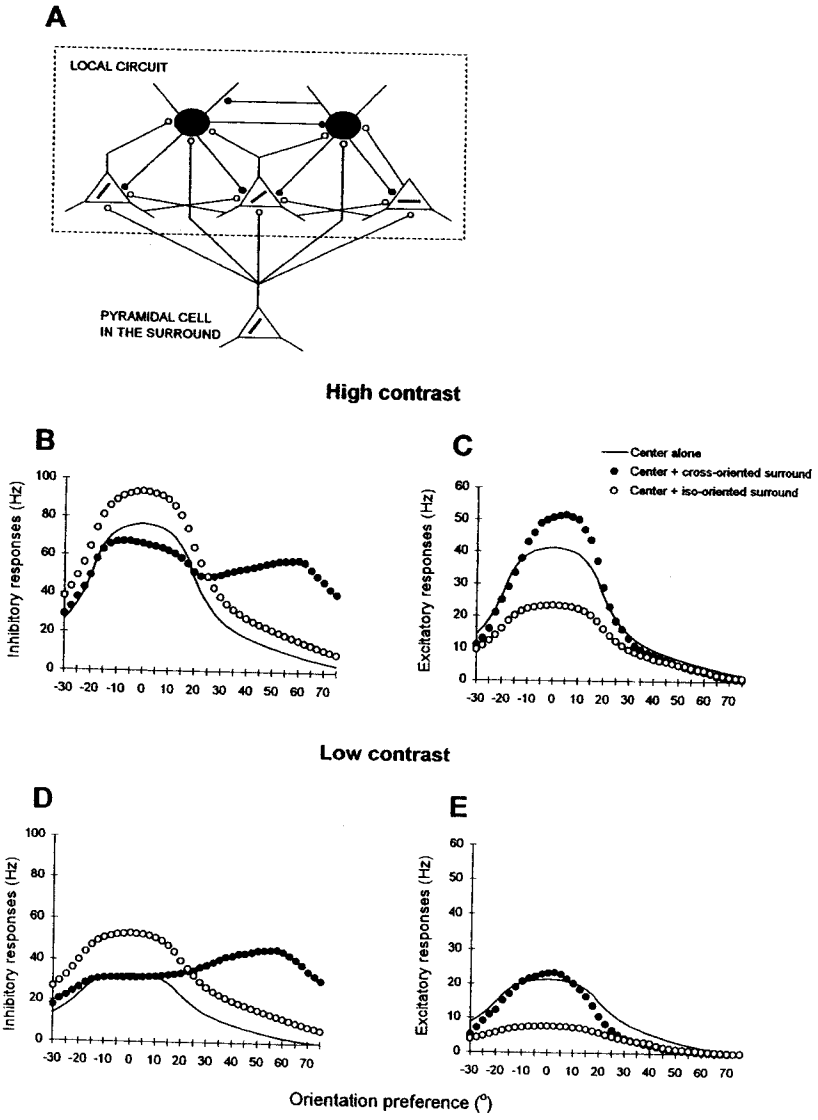

strength of excitation relative to the center-alone condition (Fig. 12-10C). This explains the iso-orientation surround suppression (Fig. 12-11A).

Low-contrast Center Stimulation

The mechanism just described is manifested when the receptive field is stimulated at high contrast. However, it becomes ineffective when the center is presented with a low-contrast stimulus. If the surround is cross-oriented at 60° and the center orientation is 0° and 15% contrast level, inhibitory neurons iso-oriented relative to the surround (i.e., preferred orientation 60°) decrease their response to suppress only weakly their postsynaptic targets, including other inhibitory cells. Indeed, Fig. 12-10D shows that, relative to the center-alone condition, inhibitory responses are suppressed to a lesser extent than in the high-contrast case. Therefore, the iso-oriented inhibitory neurons are no longer capable of sustaining the release from inhibition of the non-iso-orientation excitatory cells, and thus the total excitatory input to cortical cells does not differ substantially from the center-alone condition (Fig. 12-10E). The net effect of this interaction is the disappearance of surround cross-orientation facilitation (Fig. 12-11B), and a broader tuning of the suppressive effects.

In summary, the recurrent inhibition model demonstrates that orientation-dependent long- and short-range connections can have biphasic modulatory effects, depending on the relative orientation and contrast between center and surround. Thus, Fig. 12-11A shows that responses to the center stimulus are suppressed by an iso-oriented surround. However, responses to the same center stimulus become supraoptimal in the presence of an orthogonal or oblique surround. These results provide a good fit to the experimental data obtained in similar conditions (Levitt

FIGURE 12-10. Analysis of contrast-dependent center-surround interactions. **(A)** Schematic diagram of the interactions between representative cells in the superficial layers of V1 embedded in their local circuit (dashed rectangle). Pyramidal cells in the surround project to both excitatory (triangles) and inhibitory (filled circles) neurons. Empty circles, excitatory connections; filled circles, inhibitory connections. **(B)** The response of inhibitory cortical cells with orientation preferences between –30° and 75°. When the surround is cross-oriented (filled circles), cells oriented away from the surround orientation are released from local inhibition relative to the center-alone condition (solid line). When the surround is iso-oriented (empty circles) there is an overall increase in the local inhibition level. **(C)** The response of excitatory cortical cells with orientation preferences between –30° and 75°. When the surround is cross-oriented, the net effect of the removal of tonic inhibition from pyramidal cells in the vicinity of the 0° domain is an increase in the strength of excitation relative to the center-alone condition. When the surround is iso-oriented, there is a decrease in the response of excitatory cells relative to the center-alone condition. Center stimulus: 100% contrast level, orientation is fixed at 0° (panels C and D). **(D)** The response of inhibitory cortical cells with orientation preferences between –30 and 75°. When the surround is cross-oriented, inhibitory responses are suppressed to a lesser extent than in the high-contrast case. **(E)** The response of excitatory cortical cells with orientation preferences between –30 and 75°. When the surround is cross-oriented the total excitatory input to cortical cells does not differ substantially from the center-alone condition. Center stimulus: 15% contrast level, orientation is fixed at 0°.

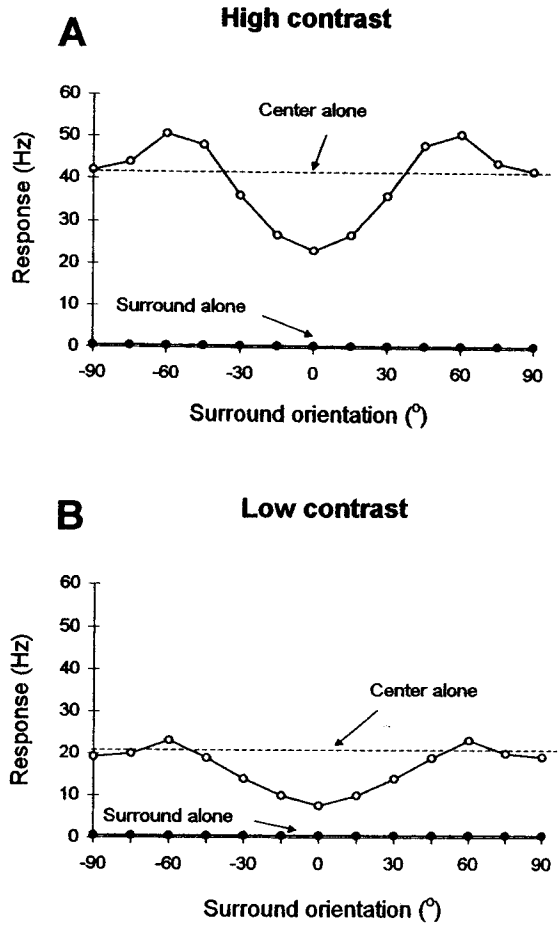

FIGURE 12-11. Contrast and orientation dependence of contextual effects (modeling results). **(A)** Model responses to the high-contrast optimal center stimulus (contrast 100%) paired with a high-contrast surround of varying orientation (empty circles) and to the surround stimulus alone (filled circles). Center contrast and surround orientation values are identical to those used by Levitt and Lund (1997). **(B)** Model responses to the low-contrast optimal center stimulus (contrast 15%) paired with a high-contrast surround of varying orientation (empty circles) and to the surround stimulus alone (filled circles). Center contrast and surround orientation values are identical to those used by Levitt and Lund (1997). Dashed lines in all panels indicate response to the optimal stimulus alone (high-center contrast value is 100% in panel A; low-center contrast value is 15% in panel B).

and Lund, 1997) (Fig. 12-9A). When the center stimulus is presented at low contrast, the facilitatory effects induced by cross-oriented surround stimuli disappear or become very small (Fig. 12-11B), and this determines a broader tuning of the suppressive effects (Levitt and Lund, 1997) (Fig. 12-9B). We have thus demonstrated that under some center-surround configurations, the responses of inhibitory

interneurons can be completely reversed: iso-oriented stimuli in the surround increase the firing rate of local inhibitory cells that further suppress their postsynaptic pyramidal cells, and cross-oriented stimuli in the surround decrease the firing rate of local inhibitory cells that further disinhibit their postsynaptic pyramidal cells. In addition, the magnitude of the disinhibitory effect decreases with reductions in the center contrast level. Thus, the recurrent inhibition model advances a clear-cut prediction: measuring the total intracellular excitatory and inhibitory synaptic responses during in vivo presentations of different center-surround configurations would yield inhibitory responses below the center-alone condition and excitatory responses above the center-alone condition when the surround is cross-oriented, and inhibitory responses above the center-alone condition and excitatory responses below the center-alone condition when the surround is iso-oriented.

SHORT-TERM PLASTICITY OF ORIENTATION TUNING INDUCED BY PATTERN ADAPTATION

INTRODUCTION

The last two sections showed that selective stimulation of the receptive field center and surround explains nonlinear contextual effects in the contrast and orientation domains. These effects arise as a consequence of spatial interactions and persist as long as the center and surround stimuli are presented together. However, if changes in the gain of local circuitry are indeed responsible for changes in the response properties of cortical neurons and if orientation selectivity is an emergent property of recurrent networks, we would predict that altering the efficacy of intracortical orientation-specific inputs would induce *changes* in the tuning properties of neurons. One way to alter the efficacy of cortical inputs to a V1 neuron is to enhance or suppress the excitability of individual or small groups of neurons. We have shown that focal iontophoresis of bicuculline or GABA to a cortical column alters the orientation tuning properties of adjacent cortical columns (Toth et al., 1997). Another way to alter intracortical inputs is to adapt a cell to a stimulus of fixed orientation. It is known that adapting neurons to a potent stimulus can reduce responses to subsequent similar stimuli. In a recent study (Dragoi et al., 2000), we examined the changes in orientation tuning using pattern adaptation (Movshon and Lennie, 1979; Saul and Cynader, 1989; Carandini et al., 1998) as the induction procedure by analyzing how the entire profile of the orientation tuning curve changes after short- and long-term adaptation to a particular stimulus orientation.

RESULTS

Single Cell Responses

In contrast to the common view of adaptation as simply a passive process of response suppression, we found that exposure to particular orientations reveals an active process of plasticity by which responses on the flank of the tuning curve

near the adapting orientation are depressed, whereas responses on the opposite flank of the tuning curve are enhanced. For instance, Fig. 12-12A shows how the preferred orientation of a representative cell changes after 2 minutes of exposure to one orientation located on one flank of the cell's tuning curve, followed by a period of recovery, subsequent adaptation to a different orientation located on the opposite flank with respect to the preferred orientation, and a final period of recovery. When the difference between the cell's preferred orientation and that of the adapting stimulus ($\Delta\theta$) is –22.5°, there is a shift in preferred orientation to the right, away from the adapting stimulus. In contrast, when the adapting stimulus is presented on the right flank of the tuning curve ($\Delta\theta = 45°$), the preferred orientation shifts to the left and then returns to the original value after 10 minutes of recovery. However, adaptation to stimuli orthogonal to the cell's preferred orientation ($\Delta\theta$ between approximately 60° and 90°) does not induce any change in preferred orientation. Figure 12-12B illustrates the behavior of one representative cell that exhibits a stimulus-dependent shift after 2 minutes of adaptation to a 22.5° stimulus, but the orientation preference remains unchanged when $\Delta\theta$ is 90°. In both postadaptation conditions, there is a decrease in response at the preadaptation preferred orientation and a broadening of tuning.

Interestingly, the shape of the orientation tuning curve undergoes profound changes when neurons are serially exposed to different adaptation periods. For instance, Fig. 12-12C,D shows one cell that exhibits significant shifts in orientation after adaptation for 10 seconds, 2 minutes, and 10 minutes to a stimulus oriented 45° away from the cell's peak orientation. Both the response reduction on the near flank (toward the adapting orientation) and facilitation on the far flank of the tuning curve (away from the adapting orientation) build up gradually in time: increasing the adaptation time from 10 seconds to 10 minutes shows a progressive depression of responses on the near flank and a progressive facilitation of responses on the far flank. For the largest adaptation period (10 minutes), we found that many cells increase their response at the new preferred orientation by a factor of 2 or more (Fig. 12-12D). The orientation at which the adapting stimulus is presented elicits weak or no responses under the various time periods (e.g., Fig. 12-12C,D). Yet adaptation induces a significant shift in optimal orientation, along with the reorganization of responses around the new preferred orientation. Thus, orientation plasticity involves an active process of network synaptic changes that lead to a new preferred orientation rather than simply a passive reduction of orientation-selective responses around the adapting orientation.

Optical Imaging Studies of Adaptation

We also investigated short-term plasticity in orientation tuning at the population level by carrying out optical imaging of intrinsic signals (Grinvald et al., 1986) from an expanse of V1 (Dragoi et al., 2000). Figure 12-13A shows three composite orientation preference maps from one animal, combining response images at eight different stimulus orientations, obtained during control, adaptation, and

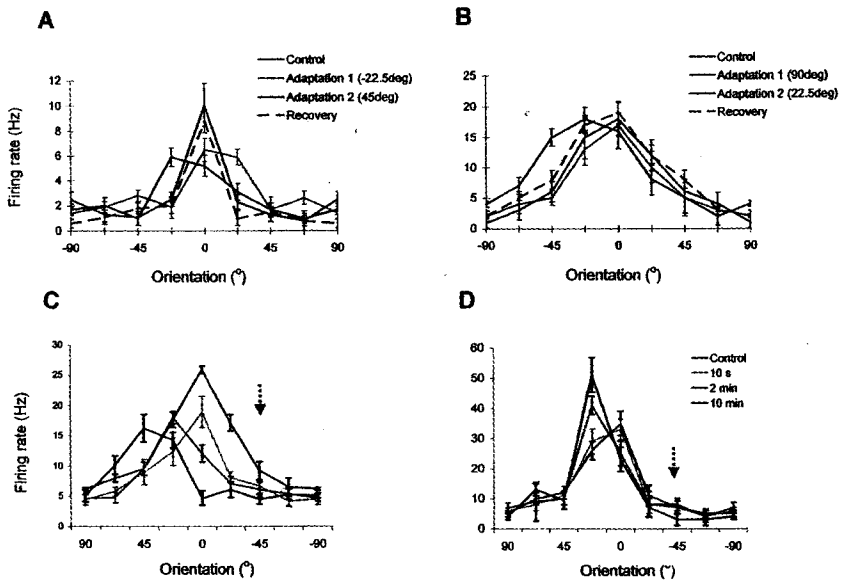

FIGURE 12-12. Plasticity of orientation tuning in V1 cells. **(A-B)** Orientation tuning curves of two representative cells that were successively adapted to two different orientations. Each graph represents orientation tuning during four conditions: control (red), adaptation to the first orientation (light blue), adaptation to the second orientation (dark blue), and recovery (red, dashed line). In our tuning curve display convention, the control optimal orientation is represented as 0°, and all subsequent tuning curves (during adaptation and recovery) are represented relative to the control condition. **(C-D)** Tuning curves of cells that show adaptation-induced response suppression on the near flank and response facilitation on the far flank. Each cell was serially exposed to different adaptation periods: 10 seconds, 2 minutes, and 10 minutes. Tuning curves were calculated in each of the four conditions: control (red), 10-second adaptation (light blue), 2-minute adaptation (blue), and 10-minute adaptation (dark blue). The adapting orientation is marked by the blue arrow. See color insert for color reproduction of this figure.

recovery conditions. The adapting orientation was fixed throughout the experiment at 135° (dark green bar in Fig. 12-13A). We determined the change in cortical responses induced by the adapting stimulus by computing the difference in orientation preference between control, adaptation, and recovery conditions for each pixel. If the adapting orientation shifts the preferred orientation of cells, pixels flanking the adapting orientation would change their vector angle away from the adapting orientation (dark green). For example, most pixels preferring 112.5° (light green) would shift toward 90° (yellow), and the 90° pixels would shift toward 67.5° (orange). At the opposite side of the adapting orientation, most pixels preferring 157.5° (light blue) would shift toward 180° (dark blue), and the 180° (or 0°) pixels would shift toward 22.5° (purple). Pixels whose orientation preference exactly matches that of the adapting stimulus (i.e., 135° [dark green] would show minimal changes in their angle; others with actual preferred orientation close to

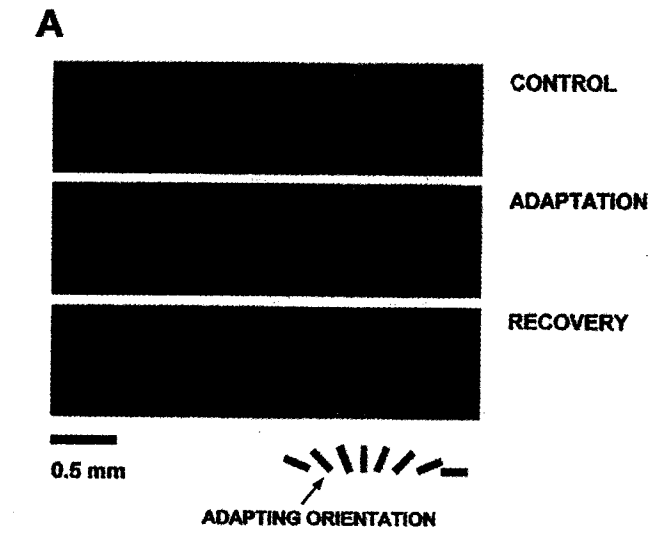
A
CONTROL
ADAPTATION
RECOVERY
0.5 mm
ADAPTING ORIENTATION
B
Control
Adaptation
Recovery
C
Change in pixel orientation (°)
30
20
10
0
-10
-20
-30
Adaptation - Control
Recovery - Control
-90 -67.5 -45 -22.5 0 22.5 45 67.5 90
Orientation range (°)

FIGURE 12-13. Changes in orientation tuning in an expanse of V1 demonstrated by optical imaging. **(A)** Composite maps of orientation angle obtained during control, adaptation, and recovery conditions. Data analysis was performed using original, unfiltered, single orientation maps in all three conditions. To obtain these composite maps we summed vectorially the response at each pixel to the eight single stimulus orientations (including both directions of motion) and displayed the resultant angle of preferred orientation in pseudocolor according to the key at bottom. Each map was smoothed using a low-pass filter, 5×5 kernel size. Adapting orientation is coded dark green. **(B)** Magnified portion from **(A)**, showing the postadaptation repulsive shift in orientation and the recovery from adaptation. Depending on the difference between pixel orientation and that of the adapting stimulus ($\Delta\theta$) orientation domains exhibit repulsive shift toward neighboring orientations: for $\Delta\theta = -22.5°$ (light green) most pixels shift toward the "yellow" domain; for $\Delta\theta = 0°$ (dark green) many pixels are unchanged and others shift either toward the "light green" or "light blue" domains; for $\Delta\theta = 22.5°$ (light blue) most pixels shift toward the "dark blue" domain. **(C)** Change in pixel orientation during adaptation and recovery. Orientation changes were calculated for all pixels in the entire map shown in **(A)** by subtracting the pixel vector angle in the control map from that of the corresponding pixel in the adaptation or the recovery map. We divided all pixels into 16 bins, which are represented, relative to the adapting orientation (135°), as the following intervals: [–90°, –78.75°], [–78.75°, –67.5°] ... [78.75°, 90°]. Each of these bins is represented on the abscissa by the lower bound of each orientation interval. The numbers of the y-axis represent the average change in pixel angle. See color insert for color reproduction of this figure.

135° [135° ± 11.25°] would also shift repulsively with respect to the adapting orientation). Finally, if the shift is reversible, all pixels should revert to their initial orientation after recovery from adaptation. Figure 12-13B shows a magnified portion from Fig. 12-13A that captures the repulsive shift in orientation during adaptation and then shows that most pixels recover to their original orientation.

Figure 12-13C demonstrates quantitatively that a repulsive shift in orientation follows adaptation. The change in orientation for each pixel during adaptation and recovery was quantified by calculating the difference between the vector angle of each pixel before and after adaptation, and before adaptation and after recovery. There is a positive change in orientation when the difference between each pixel's orientation and the adapting orientation is positive, and a negative change in orientation when the difference between each pixel's orientation and the adapting orientation is negative. Also paralleling the single-unit data, Fig. 12-13C shows that as the orientation difference increases from 0 to about ± 22.5°, the repulsive shift increases, and this effect diminishes as the orientation difference approaches ± 90°. During recovery there is a reversal toward original (control) pixel values.

These results demonstrate that the orientation-selective responses of adult V1 cells are reorganized actively and nonlinearly by the temporal context of stimulation. Previous examination of the effect of temporal context pertains to studies that have demonstrated that adapting neurons to a potent stimulus can reduce responses to subsequent similar stimuli. This property has been characterized with respect to many stimulus dimensions, such as orientation (Blakemore and Campbell, 1969; Hammond et al., 1989; Nelson, 1991; Carandini et al., 1998),

contrast (Movshon and Lennie, 1979; Ohzawa et al., 1982; Carandini and Ferster, 1997; Carandini et al., 1997), spatial frequency (Movshon and Lennie, 1979; Saul and Cynader, 1989), direction of motion (Maffei et al., 1973; Hammond et al., 1985; 1986), and velocity (Hammond et al., 1985). Saul and Cynader (1989) have demonstrated that pattern adaptation causes changes in the spatial frequency tuning of a small group of V1 neurons, an effect related to the changes in orientation preference reported here. However, it is generally assumed that in the orientation domain adaptation reduces responses at all orientations, the maximum reduction being obtained when the cell's preferred orientation and that of the adapting stimulus are the same (this property can be generalized to most stimulus attributes). A reduction of responses may result from mechanisms at the level of individual neurons, such as tonic hyperpolarization of the membrane potential of V1 cells (Carandini and Ferster, 1997), resulting possibly from synaptic depression (Abbott et al., 1997; Chance et al., 1998) or to slow hyperpolarizing Ca- and Na-activated potassium channels (Sanchez-Vives et al., 2000). The changes in orientation selectivity reported here (i.e., shifts in orientation preference by depression of responses on the near flank and facilitation of responses on the far flank) imply a network mechanism that reorganizes responses across a broad range of orientations, possibly through changes in the gain of local cortical circuits that mediate recurrent excitation and inhibition (Douglas et al., 1995; Somers et al., 1995a, 1998) and include disinhibitory mechanisms (Dragoi and Sur, 2000). For example, if the local cortical circuit includes broadly tuned orientation inhibition, hyperpolarization of neurons representing the adapting orientation could cause disinhibition of responses on the far flank of the tuning curve in the recorded neuron, an effect that could be further amplified via local excitatory interactions.

CONCLUDING REMARKS

The models and data presented here constitute a powerful argument for the proposal that orientation selectivity is generated and modulated by a combination of thalamocortical inputs to VI neurons and intracortical processing. Cortical neurons are embedded in diverse circuitry: each neuron receives not only excitatory thalamocortical inputs but also excitatory intracortical input from local neurons, inhibitory input from local interneurons, and excitatory long-range input from distant neurons. It would be surprising indeed if these diverse components of circuitry did not find expression in the responses of V1 cells. In fact these complex inputs are integrated in nonlinear fashion, and this integration is expressed in the various nonlinear response properties of V1 cells. A final feature of V1 neurons that is difficult to explain by feedforward connections alone is their responses to subjective or illusory contours and the systematic mapping of subjective contour orientation within V1 (Sheth et al., 1996). A model involving iso-orientation intracortical excitation to amplify LGN responses at line ends is able to reproduce the subjective contour responses and representations within V1

(Kalarickal and Sur, 1999). These response properties include orientation selectivity, modulation of orientation selective responses by spatial context or surround stimuli, and modulation as well by temporal context or pattern adaptation. A linear feedforward model of orientation selectivity was adequate for explaining the simplest, first-order, responses of V1 neurons, at a time when responses to unitary stimuli presented within the receptive field center were regarded as the only significant property of V1 cells. As our appreciation of the complexity of V1 responses has increased, our models for explaining such complexity need to keep pace with the known richness of circuitry. A description of V1 circuits that incorporates this knowledge has to include recurrent excitation and inhibition, and indeed such models provide a natural explanation for many of the complex nonlinear responses of V1 cells. They also provide hope that as we understand and incorporate even more aspects of cortical connections, we shall indeed be able to unravel the mechanisms behind even complex emergent properties of cortical neurons.

ACKNOWLEDGMENTS

We thank Jennifer Vazquez for help with preparing the manuscript. Supported by fellowships from Merck Inc. and the McDonnell-Pew Foundation (V.D.), and grants from the NIH (M.S., D.S. to Edward H. Adelson).

REFERENCES

Abbott, L. F., Varela, J. A., Sen, K., and Nelson, S. B. (1997). Synaptic depression and cortical gain control. *Science* **275,** 220–224.

Ahmed, B. A., Anderson, J. C., Douglas, R. J., Martin, K. A. C., and Nelson, J. C. (1994). Polyneuronal innervation of spiny stellate neurons in cat visual cortex. *J. Comp. Neurol.* **341,** 39–49.

Albrecht, D. G., and Geisler, W. (1991). Motion selectivity and the contrast-response function of simple cells in the striate cortex. *Vis. Neurosci.* **7,** 531–546.

Albrecht, D. G., and Hamilton, D. B. (1982). Striate cortex of monkey and cat: contrast response function. *J. Neurosci.* **48,** 217–237.

Alonso, J. M., Usrey, W. M., and Reid, R. C. (1996). Precisely correlated firing in cells of the lateral geniculate nucleus. *Nature* **383,** 815–819.

Anderson, J. C., Douglas, R. J., Martin, K. A. C., and Nelson, J. C. (1994a). Synaptic output of physiologically identified spiny stellate neurons in cat visual cortex. *J. Comp. Neurol.* **341,** 16–24.

Anderson, J. C., Douglas, R. J., Martin, K. A. C., and Nelson, J. C. (1994b). Map of the synapses formed with the dendrites of spiny stellate neurons of cat visual cortex. *J. Comp. Neurol.* **341,** 25–38.

Anderson, J. S., Carandini, M., and Ferster, D. (2000a). Orientation tuning of input conductance, excitation, and inhibition in cat primary visual cortex. *J. Neurophysiol.* **84,** 909–926.

Anderson, J., Lampl, I., Reichova, I., Carandini, M., and Ferster, D. (2000b). Stimulus dependence of two-state fluctuations of membrane potential in cat visual cortex. *Nat. Neurosci.* **3,** 617–621.

Beaulieu, C., and Somogyi, P. (1990). Targets and quantitative distribution of GABAergic synapses in the visual cortex of the cat. *Eur. J. Neurosci.* **2,** 296–303.

Ben-Yishai, R., Bar-Or, R. L., and Sompolinsky, H. (1995). Theory of orientation tuning in visual cortex. *Proc. Natl. Acad. Sci. U.S.A.* **92,** 3844–3848.

Berman, N. J., Douglas, R. J., Martin, K. A. C., and Whitteridge, D. (1991). Mechanisms of inhibition in cat visual cortex. *J. Physiol.* **440,** 697–722.

Bishop, P. O., Coombs, J. S., and Henry, G. H. (1973). Receptive fields of simple cells in the cat striate cortex. *J. Physiol.* **231,** 31–60.

Blakemore, C., and Tobin, E. A. (1972). Lateral inhibition between orientation detectors in the cat's visual cortex. *Exp. Brain Res.* **15,** 439–440.

Blakemore, C. and Campbell, F. W. J. (1969). Adaptation to spatial stimuli. *J. Physiol. (Lond.)* **200,** 11P.

Blomfield, S. (1974). Arithmetical operations performed by nerve cells. *Brain Res.* **9,** 115–124.

Bonds, A. B. (1989). Role of inhibition in the specification of orientation selectivity of cells in the cat striate cortex. *Vis. Neurosci.* **2,** 41–55.

Bonds, A. B. (1991). Temporal dynamics of contrast gain in single cells of the cat striate cortex. *Vis. Neurosci.* **6,** 239–255.

Bonds, A. B. (1993). The encoding of cortical contrast gain control. In: Contrast sensitivity (Shapley, R. M., and Lam, D-K., Eds.), pp. 215–230, Cambridge, MIT Press.

Borg-Graham, L. J., Monier, C., and Fregnac, Y. (1998). Visual input evokes transient and strong shunting inhibition in visual cortical neurons. *Nature* **393,** 369–373.

Born, R. T., and Tootell, R. B. H. (1991). Single-unit and 2-deoxyglucose studies of side inhibition in macaque striate cortex. *Proc. Natl. Acad. Sci. U.S.A.* **88,** 7071–7075.

Bosking, W. H., Zhang, Y., Schofield, B., and Fitzpatrick, D. (1997). Orientation selectivity and the arrangement of horizontal connections in tree shrew striate cortex. *J. Neurosci.* **17,** 2112–2127.

Bullier, J., Hupe, J. M., James, A., and Girard, P. (1996). Functional interactions between areas V1 and V2 in the monkey. *J. Physiol. (Paris)* **90,** 217–220.

Bush, P. C., and Sejnowski, T. J. (1994). Effects of inhibition and dendritic saturation in simulated neocortical pyramidal cells. *J. Neurophysiol.* **71,** 2183–2193.

Carandini, M., and Heeger, D. J. (1994). Summation and division by neurons in primate visual cortex. *Science* **264,** 1333–1336.

Carandini, M., and Ringach, D. (1997). Predictions of a recurrent model of orientation selectivity. *Vis. Res.* **37,** 3061–3071.

Carandini, M., and Ferster, D. (2000). Orientation tuning of membrane potential and firing rate in cat primary visual cortex. *J. Neurosci.* **20,** 470–484.

Carandini, M., Barlow, H. B., O'Keefe, O. P., Poirson, A. B., and Movshon, J. A. (1997). Adaptation to contingencies in macaque primary visual cortex. *Phil. Trans. R. Soc. Lond. B.* **352,** 1149–1154.

Carandini, M., and Ferster, D. (1997). A tonic hyperpolarization underlying contrast adaptation in cat visual cortex. *Science* **276,** 949.

Carandini, M., Movshon, J. A., and Ferster, D. (1998). Pattern adaptation and cross-orientation interactions in the primary visual cortex. *Neuropharmacology* **37,** 501.

Chance, F. S., and Abbott, L. F. (2000). Divisive inhibition in recurrent networks. *Network* **11,** 119–129.

Chance, F. S., Nelson, S. B., and Abbott, L.F. (1999). Complex cells as cortically amplified simple cells. *Nat. Neurosci.* **2,** 277–282.

Chance, F. S., Nelson, S. B., and Abbott L. F. (1998). Synaptic depression and the temporal response characteristics of V1 cells. *J. Neurosci.* **18,** 4785.

Chapman, B., Zahs, K. R., and Stryker, M. P. (1991). Relation of cortical cell orientation selectivity to alignment of receptive fields of the geniculocortical afferents that arborize within a single orientation column in ferret visual cortex. *J. Neurosci.* **11,** 1347–1358.

Chino, Y. M., and Kaplan, E. (1988). Abnormal orientation bias of LGN neurons in strabismic cats. *Invest. Ophthalmol. Vis. Sci.* **29,** 644–648.

Chung, S., and Ferster, D. (1998). Strength and orientation tuning of thalamic input to simple cells revealed by electrically evoked cortical suppression. *Neuron* **20,** 1177–1189.

Connors, B. W., Gutnick, M. J., and Prince, D. A. (1982). Electrophysiological properties of neocortical neurons in vitro. *J. Neurophysiol.* **48,** 1302–1320.

Creutzfeldt, O. D., Kuhnt, U., and Benevento, L. A. (1974a). An intracellular analysis of visual cortical neurons to moving stimuli: responses in a cooperative neuronal network. *Exp. Brain Res.* **21,** 251–274.

Creutzfeldt, O. D., Innocenti, G., and Brooks, D. (1974b). Vertical organization in the visual cortex (area 17). *Exp. Brain Res.* **21,** 315–336.

Crook, J. M., and Eysel, U. T. (1992). GABA-induced inactivation of functionally characterized sites in cat visual cortex (area 18): effects on orientation tuning. *J. Neurosci.* **12,** 1816–1825.

Das, A. (1996). Orientation in visual cortex: a simple mechanism emerges. *Neuron* **16,** 477.

Dean, A. F., and Tolhurst, D. J. (1986). Factors influencing the temporal phase of response to bar and grating stimuli for simple cells in the cat striate cortex. *Exp. Brain Res.* **62,** 143–151.

DeAngelis, G. C., Robson, J. G., Ohzawa, I., and Freeman, R. D. (1992). Organization of suppression in receptive fields of neurons in cat visual cortex. *J. Neurophysiol.* **68,** 144–163.

DeAngelis, G. C., Freeman, R. D., and Ohzawa, I. (1994). Length and width tuning of neurons in the cat's primary visual cortex. *J. Neurophysiol.* **71,** 347–374.

DeAngelis, G. C., Ohzawa, I., and Freeman, R. D. (1995). Receptive field dynamics in the central visual pathways. *Trends Neurosci.* **18,** 451–458.

Dehay, C., Douglas, R. J., Martin, K. A. C, and Nelson, C. (1991). Excitation by geniculocortical synapses is not "vetoed" at the level of dendritic spines in cat visual cortex. *J. Physiol.* **440,** 723–734.

Douglas, R. J., Martin, K. A. C., and Whitteridge, D. (1991). An intracellular analysis of the visual responses of neurones in cat visual cortex. *J. Physiol.* **44,** 659–696.

Douglas, R. J., Koch, C., Mahowald, M., Martin, K. A. C., and Suarez, H. H. (1995). Recurrent excitation in neocortical circuits. *Science* **269,** 981–985.

Douglas, R. J., and Martin, K. A. C. (1991a). Opening the grey box. *Trends Neurosci.* **14,** 286–293.

Douglas, R. J., and Martin, K. A. C. (1991b). A functional microcircuit for cat visual cortex. *J. Physiol.* **440,** 735–769.

Douglas, R. J., Martin, K. A. C., and Whitteridge, D. (1988). Selective responses of visual cortical neurones do not depend on shunting inhibition. *Nature* **332,** 642–644.

Douglas, R. J., Martin, K. A. C., and Whitteridge, D. (1989). A canonical microcircuit for neocortex. *Neural Comp.* **1,** 480–488.

Dragoi, V., Sharma, J., Miller, E. K. M., and Sur M. (1999). Dynamics of orientation adaptation in awake monkey primary visual cortex revealed by reverse correlation. *Soc. Neurosci. Abstr.* **25,** 1548.

Dragoi, V., and Sur, M. (2000). Dynamic properties of recurrent inhibition in primary visual cortex: contrast and orientation dependence of contextual effects. *J. Neurophysiol.* **83,** 1019–1030.

Dragoi, V., Sharma, J., and Sur, M. (2000). Adaptation-induced plasticity in adult visual cortex. *Neuron* (in press).

Dragoi, V., Sharma, J., and Sur, M. (2000). Adaptation-induced plasticity of orientation tuning in adult visual cortex. *Neuron.* **28,** 287–298.

Elias, S., and Grossberg, S. (1975). Pattern formation, contrast control, and oscillations in the short-term memory of shunting on-center off-surround networks. *Biol. Cybern.* **20,** 69–98.

Enroth-Cugell, C., Robson, J. G., Schweizer-Tong, D. E., and Watson, A. B. (1983). Spatio-temporal interactions in cat retinal ganglion cells showing linear spatial summation. *J. Physiol.* **341,** 279–307.

Eysel, U. T., Crook, J. M., and Machemer, H. F. (1990). GABA-induced remote inactivation reveals cross-orientation inhibition in the cat striate cortex. *Exp. Brain Res.* **80,** 626–630.

Ferster, D. (1986). Orientation selectivity of synaptic potentials in neurons of cat primary visual cortex. *J. Neurosci.* **6,** 1284–1301.

Ferster, D. (1987). Origin of orientation-selective EPSPs in simple cells of the cat visual cortex. *J. Neurosci.* **7,** 1780–1791.

Ferster, D. (1988). Spatially opponent excitation and inhibition in simple cells of the cat visual cortex. *J. Neurosci.* **8,** 1172–1180.

Ferster, D. (1994). Linearity of synaptic interactions in the assembly of receptive fields in cat visual cortex. *Curr. Opin. Neurobiol.* **4,** 563–568.

Ferster, D., and Koch, C. (1987). Neuronal connections underlying orientation selectivity in cat visual cortex. *Trends Neurosci.* **10,** 487–492.

Ferster, D., and Jagadeesh, B. (1992). EPSP-IPSP interactions in cat visual cortex studied with in vivo whole-cell patch recording. *J. Neurosci.* **12,** 1262–1274.

Ferster, D., Chung, S., and Wheat, H. (1996). Orientation selectivity of thalamic input to simple cells of cat visual cortex. *Nature* **380,** 249–252.

Ferster, D., and Miller, K. D. (2000). Neural mechanisms of orientation selectivity in the visual cortex. *Annu. Rev. Neurosci.* **23,** 441–471.

Field, D. J., Hayes, A., and Hess, R. F. (1993). Contour integration by the human visual system: evidence for a local association field. *Vis. Res.* **33,** 173–193.

Fregnac, Y., and Debanne, D. (1993). Potentiation and depression in visual cortical neurons: a functional approach to synaptic plasticity. In: 'Brain mechanisms of perception and memory: from neuron to behavior' (T. Ono, L. Squire, M. E. Raichle, D. I. Perrett, and M. Fukuda, Eds.), pp. 533–561. Oxford, UK, Oxford University Press.

Freund, T. F., Martin, K. A. C., Somogyi, P., and Whitteridge, D. (1985). Innervation of cat visual areas 17 and 18 by physiologically identified X- and Y-type thalamic afferents. II. Identification of postsynaptic targets by GABA immunocytochemistry and golgi impregnation. *J. Comp. Neurol.* **242,** 275–291.

Fries, W., Albus, K., and Creutzfeldt, O. D. (1977). Effects of interacting visual patterns on single cell responses in cat's striate cortex. *Vis. Res.* **17,** 1001–1008.

Gabbott, P. L. A., and Somogyi, P. (1986). Quantitative distribution of GABA-immunoreceptive neurons in the visual cortex (area 17) of the cat. *Exp. Brain Res.* **61,** 323–331.

Galarreta, M., and Hestrin, S. (1998). Frequency-dependent synaptic depression and the balance of excitation and inhibition in the neocortex. *Nat. Neurosci.* **1,** 587–594.

Gardner, J. L., Anzai, A., Ohzawa, I., and Freeman, R. D. (1999). Linear and nonlinear contributions to orientation tuning of simple cells in the cat's striate cortex. *Vis. Neurosci.* **16,** 1115–1121.

Ghose, G. M., Freeman, R. D., and Ohzawa, I. (1994). Local intracortical connections in the cat's visual cortex: postnatal development and plasticity. *J. Neurophysiol.* **72,** 1290–1303.

Gil, Z., Connors, B. W., and Amitai, Y. (1999). Efficacy of thalamocortical and intracortical synaptic connections: quanta, innervation, and reliability. *Neuron* **23,** 385–397.

Gilbert, C. D. (1992). Horizontal integration and cortical dynamics. *Neuron* **9,** 1–13.

Gilbert, C. D., Das, A., Ito, M., Kapadia, M., and Westheimer, G. (1996). Spatial integration and cortical dynamics. *Proc. Natl. Acad. Sci. U.S.A.* **93,** 615–622.

Gilbert, C. D., and Wiesel, T. N. (1983). Clustered intrinsic connections in cat visual cortex. *J. Neurosci.* **3,** 1116–1133.

Gilbert, C. D., and Wiesel, T. N. (1989). Columnar specificity of intrinsic horizontal and corticocortical connections in cat visual cortex. *J. Neurosci.* **9,** 2432–2442.

Gilbert, C. D., and Wiesel, T. N. (1979). Morphology and intracortical projections of functionally identified neurons in cat visual cortex. *Nature* **280,** 120–125.

Gilbert, C. D., and Wiesel, T. N. (1990). The influence of contextual stimuli on the orientation selectivity of cells in primary visual cortex of the cat. *Vis. Res.* **30,** 1689–1701.

Grinvald, A., Lieke, E. E., Frostig, R. D., Gilbert, C. D., and Wiesel, T. N. (1986). Functional architecture of cortex revealed by optical imaging of intrinsic signals. *Nature.* **324,** 361–364.

Grinvald, A., Lieke, E. E., Frostig, R. D., and Hildesheim, R. (1994). Cortical point-spread function and long-range lateral interactions revealed by real-time optical imaging of macaque monkey primary visual cortex. *J. Neurosci.* **14,** 2545–2568.

Grossberg, S. (1973). Contour enhancement, short-term memory, and constancies in reverberating neural networks. *Studies Appl. Math.* **52,** 217–257.

Grossberg, S. (1983). The quantized geometry of visual space: the coherent computation of depth, form, and lightness. *Behav. Brain Sci.* **6,** 625–692.

Grossberg, S., and Mingolla, E. (1985). Neural dynamics of perceptual grouping: textures, boundaries, and emergent segmentations. *Perception Psychophysics* **38,** 141–171.

Grossberg, S., and Olson, S. J. (1994). Rules for the cortical map of ocular dominance and orientation columns. *Neural Networks* **7,** 883–894.

Gulyas, B., Orban, G. A., Duysens, J., and Maes, H. (1987). The suppressive influence of moving textured backgrounds on responses of cat striate neurons to moving bars. *J. Neurophysiol.* **57,** 1767–1791.

Hammond, P., Mouat G. S., and Smith, A. T. (1985). Motion after-effects in cat striate cortex elicited by moving gratings. *Exp. Brain Res.* **60,** 411–416.

Hammond, P., Mouat G. S., and Smith, A. T. (1986). Motion after-effects in cat striate cortex elicited by moving texture. *Vis. Res.* **26,** 1055–1060.

Hammond, P., Pomfrett, C. J., and Ahmed, B. (1989). Neural motion after-effects in the cat's striated cortex: Orientation selectivity. *Vision Res. 29,* 1671–1683.

Hartline, H. K. (1940). The receptive fields of optic nerve fibers. *Am. J. Physiol.* **130,** 700–711.

Hata, Y., Tsumoto, T., Sato, H., Hagihara, K., and Tamura, H. (1988). Inhibition contributes to orientation selectivity in visual cortex of cat. *Nature* **335,** 815–817.

Heeger, D. J. (1992). Normalization of cell responses in cat striate cortex. *Vis. Neurosci.* **9,** 181–197.

Heeger, D. J. (1993). Modeling simple-cell direction selectivity with normalized, half-squared, linear operators. *J. Neurophysiol.* **70,** 1885–1898.

Hess, R., and Murata, K. (1974). Effects of glutamate and GABA on specific response properties of neurons in the visual cortex. *Exp. Brain Res.* **21,** 285–297.

Hestrin, S. (1992). Activation and desensitization of glutamate-activated channels mediating fast excitatory synaptic currents in the visual cortex. *Neuron* **9,** 991–999.

Hirsch, J. A. (1995). Synaptic integration in layer IV of the ferret striate cortex. *J. Physiol.* **483,** 183–199.

Hirsch, J. A., Alonso, J. M., Reid, R. C., and Martinez, L. (1998). Synaptic integration in striate cortical simple cells. *J. Neurosci.* **18,** 9517–9528.

Hirsch, J. A., Gilbert, C. D. (1991). Synaptic physiology of horizontal connections in the cat's visual cortex. *J. Neurosci.* **11,** 1800–1809.

Horton, J. C., and Sherk, H. (1984). Receptive field properties in the cat's lateral geniculate nucleus in the absence of on-center retinal input. *J. Neurosci.* **4,** 374–380.

Hubel, D. H., and Wiesel, T. N. (1962). Receptive fields, binocular interaction and functional architecture in the cat's visual cortex. *J. Physiol.* **165,** 559–568.

Hubel, D. H., and Wiesel, T. N. (1965). Receptive fields and functional architecture in two non-striate visual areas. *J. Neurophysiol.* **41,** 229–289.

Hubel, D. H., and Wiesel, T. N. (1977). Functional architecture of macaque monkey visual cortex. *Proc. R. Soc. (London) B* **198,** 1–59.

Humphrey, A. L., Sur, M., Uhlrich, D. J., and Sherman, S. M. (1985). Projection patterns of individual x-and y-cell axons from the lateral geniculate nucleus to cortical area 17 in the cat. *J. Comp. Neurol.* **233,** 159–189.

Jagadeesh, B., and Ferster, D. (1990). Receptive field lengths in cat striate cortex can increase with decreasing stimulus contrast. *Soc. Neurosci. Abstr.* **16,** 130.11.

Jagadeesh, B. (1993). The construction of receptive field properties of cells in the cat visual cortex from the synaptic inputs to the cortex. Ph.D. Dissertation. Northwestern University.

Jagadeesh, B., Wheat, H. S., and Ferster, D. (1993). Linearity of summation of synaptic potentials underlying direction selectivity of simple cells of the cat visual cortex. *Science* **262,** 1901–1904.

Jones, J. P., and Palmer, L. A. (1987). The two-dimensional spatial structure of simple receptive fields in cat striate cortex. *J. Neurophysiol.* **58,** 1187–1211.

Kalarickal, G. J., and Sur, M. (1999). Modeling orientation tuning of cortical neurons to subjective contours. *Soc. Neurosci. Abstr.* **25,** 677.

Kamphuis, W., and Lopez da Silva, F. H. (1990). The kindling model of epilepsy: the role of GABAergic inhibition. *Neurosci. Res. Commun.* **6,** 1–10.

Kapadia, M. K., Ito, M., Gilbert, C. D., and Westheimer, G. (1995). Improvement in visual sensitivity by changes in local context: parallel studies in human observers and in V1 of alert monkeys. *Neuron* **15,** 843–856.

Kaplan, E., Purpura, K., and Shapley, R. M. (1987). Contrast affects the transmission of visual information through the mammalian lateral geniculate nucleus. *J. Physiol.* **391,** 267–288.

Kisvarday, Z. F., Martin, K. A. C., Fruend, T. F., Maglоczky, Z., Whitteridge, D., and Somogyi, P. (1986). Synaptic targets of HRP-filled layer III pyramidal cells in the cat striate cortex. *Exp. Brain Res.* **64,** 541–552.

Kisvarday, Z. F., Beaulieu, C., and Eysel, U. T. (1993). Network of GABAergic large basket cells in cat visual cortex (area 18): implication for lateral disinhibition. *J. Comp. Neurol.* **327,** 398–415.

Knierim, J. J., and Van Essen, D. C. (1992). Neuronal responses to static texture patterns in area V1 of the alert macaque monkey. *J. Neurophysiol.* **67,** 961–980.

Koch, C., Douglas, R. J., and Wehmeier, U. (1990). Visibility of synaptically induced conductance changes: Theory and simulations of anatomically characterized cortical pyramidal cells. *J. Neurosci.* **10,** 1728–1744.

Koch, C., and Poggio, T. (1985). The synaptic veto mechanism: does it underlie direction and orientation selectivity in the visual cortex? In "Models of the visual cortex" (D. R. Rose, and V. G. Dobson, Ed.), pp. 408–419, New York, J. Wiley.

Kohonen, T. (1984). *Self-organization and associative memory.* New York, Springer-Verlag.

Komatsu, Y., Nakajima, S., Toyama, K., and Fetz, E. (1988). Intracortical connectivity revealed by spike-triggered averaging in slice preparations of cat visual cortex. *Brain Res.* **442,** 359–362.

Kuffler, S. W. (1953). Discharge patterns and functional organization of the mammalian retina. *J. Neurophysiol.* **16,** 37–68.

LeVay, S. (1986). Synaptic organization of claustral and geniculate afferents to the visual cortex of the cat. *J. Neurosci.* **6,** 3564–3575.

Levitt, J. B., and Lund, J. S. (1997). Contrast dependence of contextual effects in primate visual cortex. *Nature* **387,** 73–76.

Li, C. Y., and Creutzfeldt, O. D. (1984). The representation of contrast and other stimulus parameters by single neurons in area 17 of the cat. *Pflugers Arch.* **401,** 304–314.

Linsenmeier, R. A., Frishman, L. J., Jakiela, H. G., and Enroth-Cugell, C. (1982). Receptive field properties of X and Y cells in the cat retina derived from contrast sensitivity measurements. *Vis. Res.* **22,** 1173–1183.

Livingston, M. S., and Hubel, D. H. (1984). Specificity of intrinsic connections in primate primary visual cortex. *J. Neurosci.* **4,** 2830–2835.

Lund, J. S., Yoshioka, T., and Levitt, J. B. (1993). Comparison of intrinsic connectivity in different areas of macaque monkey cerebral cortex. *Cerebral Cortex* **3,** 148–162.

Lund, J. S., Wu, Q., Hadingham, P. T., and Levitt, J. B. (1995). Cells and circuits contributing to functional properties in area V1 of macaque monkey cerebral cortex: bases for neuroanatomically realistic models. *J. Anat.* **187,** 563–581.

Maffei, L., and Fiorentini, A. (1976). The unresponsive regions of visual cortical receptive fields. *Vis. Res.* **16,** 1131–1139.

Maffei, L., Fiorentini, A., and Bisti, S. (1973). Neural correlate of perceptual adaptation to gratings. *Science.* **182,** 1036–1038.

Malach, R., Amir, Y., Harel, M., and Grinvald, A. (1993). Relationship between intrinsic connections and functional architecture revealed by optical imaging and in vivo targeted biocytin injections in primate striate cortex. *Proc. Natl. Acad. Sci. U.S.A.* **90,** 10469–10473.

Malpeli, J. G. (1983). Activity of cells in area 17 of the cat in absence of input from layer A of lateral geniculate nucleus. *J. Neurophysiol.* **49,** 595–610.

Malpeli, J. G., Lee, C., Schwark, H. D., and Weyand, T. G. (1986). Cat area 17. I. Pattern of thalamic control of cortical layers. *J. Neurophysiol.* **56,** 1062–1073.

Martin, K. A. C. (1988). From single cells to simple circuits in the cerebral cortex. *Q. J. Exp. Physiol.* **73,** 637–702.

Martin, K. A. C., and Whitteridge, D. (1984). Form, function, and intracortical projections of spiny neurons in the striate visual cortex of the cat. *J. Physiol.* **353,** 463–504.

Mason, A., Nicoll, A., and Stratford, K. (1991). Synaptic transmission between individual pyramidal neurons of the rat visual cortex in vitro. *J. Neurosci.* **11,** 72–84.

Matsubara, J. A., Cynader, M. S., and Swindale, N. V. (1987). Anatomical projections and physiological correlates of the intrinsic connections in cat area 18. *J. Neurosci.* **7,** 1428–1446.

McCormick, D. A., Connors, B. W., Lighthall, J. W., and Prince, D. A. (1985). Comparative electrophysiology of physiology of pyramidal and sparsely spiny stellate neurons of the neocortex. *J. Neurophysiol.* **54,** 782–806.

McGuire, B. A., Gilbert, C. D., Rivlin, P. K., and Wiesel, T. N. (1991). Targets of horizontal connections in macaque primary visual cortex. *J. Comp. Neurol.* **305,** 370–392.

McLaughlin, D., Shapley, R., Shelley, M., and Wielaard, D. J. (2000). A neuronal network model of macaque primary visual cortex (V1): Orientation selectivity and dynamics in the input layer 4Calpha. *Proc. Natl. Acad. Sci. U.S.A.* **97,** 8087–8092.

Michalski, A., Gerstein, G. I., Czarkowska, J., and Tarnecki, R. (1983). Interactions between cat striate cortex neurons. *Exp. Brain. Res.* **51,** 97–107.

Miller, K. D. (1992). Development of orientation columns via competition between on- and off-center inputs. *Neuroreport* **3,** 73–76.

Miller, K. D. (1994). A model for the development of simple cell receptive fields and the ordered arrangement of orientation columns through activity-dependent competition between on- and off-center inputs. *J. Neurosci.* **14,** 409–441.

Morrone, M. C., Burr, D. C., and Maffei, L. (1982). Functional implications of cross—orientation inhibition of visual cortical cells. I. Neurophysiological evidence. *Proc. R. Soc. Lond. B* **216,** 335–354.

Mountcastle, V. B. (1978). An organizing principle for the cerebral function: the unit module and the distributed system. In: 'The Mindful Brain' (G. M. Edelman, and V. B. Mountcastle, Eds.), pp. 7–50. Cambridge, MA, MIT Press.

Movshon, J. A., Thompson, I. D., and Tolhurst, D. J. (1978). Spatial summation in the receptive fields of simple cells in the cat's striate cortex. *J. Physiol.* **283,** 53–77.

Movshon, A., and Lennie, P. (1979). Pattern-selective adaptation in visual cortical neurones. *Nature* **278,** 850.

Murphy, P. C., Duckett, S. G., and Sillito A. M. (1999). Feedback connections to the lateral geniculate nucleus and cortical response properties. *Science* **286,** 1552–1554.

Nelson, J. I., and Frost, B. J. (1978). Orientation-selective inhibition from beyond the classic visual receptive field. *Brain Res.* **139,** 359–365.

Nelson, J. I., and Frost, B. J. (1985). Intracortical facilitation among co-oriented, co-axially aligned simple cells in cat striate cortex. *Exp. Brain Res.* **61,** 54–61.

Nelson, S. B. (1991). Temporal interactions in the cat visual system. III. Pharmacological studies of cortical suppression suggest a presynaptic mechanism. *J. Neurosci.* **11,** 369–380.

Nelson, S. B., Toth, L. J., Sheth, B., and Sur, M. (1994). Orientation selectivity of cortical neurons persists during intracellular blockade of inhibition. *Science* **265,** 774–777.

Ohzawa, I., Sclar, G., and Freeman, R. D. (1982). Contrast gain control in the cat visual cortex. *Nature.* **298,** 266–268.

Orban, G. A., Kato, H., and Bishop, P. O. (1979). Dimensions and properties of end-zone inhibitory areas in receptive fields of hypercomplex cells in cat striate cortex. *J. Neurophysiol.* **42,** 833–849.

Orban, G. A. (1984). *Neuronal operations in the visual cortex.* Berlin, Springer.

Pei, X., Vidyasagar, T. R., Volgushev, M., and Creutzfeldt, O. D. (1994). Receptive field analysis and orientation selectivity of postsynaptic potentials of simple cells in cat visual cortex. *J. Neurosci.* **14,** 7130–7140.

Peichl, L., and Wassle, H. (1979). Size, scatter and coverage of ganglion cell receptive field centers in the cat retina. *J. Physiol.* **291,** 117–141.

Peters, A., and Payne, B. R. (1993). Numerical relationships between geniculocortical afferents and pyramidal cell modules in cat primary visual cortex. *Cerebral Cortex* **3,** 69–78.

Peters, A., and Yilmaz, E. (1993). Neuronal organization in area 17 of cat visual cortex. *Cerebral Cortex* **3,** 49–68.

Peters, A., and Sethares, C. (1991). Organization of pyramidal neurons in area 17 of monkey visual cortex. *J. Comp. Neurol.* **306,** 1–23.

Peters, A., and Sethares, C. (1996). Myelinated axons and the pyramidal cell modules in monkey primary visual cortex. *J. Comp. Neurol.* **365,** 232–255.

Poggio, T., and Reichardt, W. E. (1976). Visual control of orienting behavior in the fly. II. Towards the underlying neural interactions. *Q. Rev. Biophys.* **9,** 377–438.

Polat, U., and Sagi, D. (1993). Lateral interactions between spatial channels: suppression and facilitation revealed by lateral masking experiments. *Vis. Res.* **33,** 993–999.

Polat, U., Mizobe, K., Pettet, M. W., Kasamatsu, T., and Morcia, A. M. (1998). Collinear stimuli regulate visual responses depending on cell's contrast threshold. *Nature* **391,** 580–584.

Press, W. H., Flannery, B. P., Teukolsky, S. A., and Vetterling, W. T. (1992). *Numerical recipes in C: the art of scientific computing,* 2nd ed., pp. 566–597. Cambridge, Cambridge University Press.

Pugh, M. C., Ringach, D. L., Shapley, R., and Shelley, M. J. (2000). Computational modeling of orientation tuning dynamics in monkey primary visual cortex *J. Comput. Neurosci.* **8,** 143–159.

Rakic, P. (1988). Specification of cerebral cortical areas. *Science* **241,** 170–176.

Ramoa, A. S., Shadlen, M., Skottun, B. C., and Freeman, R. D. (1986). A comparison of inhibition in orientation and spatial frequency selectivity of cat visual cortex. *Nature* **321,** 237–239.

Reid, R. C., and Alonso, J. M. (1995). Specificity of monosynaptic connections from thalamus to visual cortex. *Nature* **387,** 281–284.

Reid, R. C., Soodak, R. E., and Shapley, R. M. (1987). Linear mechanisms of direction selectivity in simple cells of cat striate cortex. *Proc. Natl. Acad. Sci. U.S.A.* **84,** 8740–8744.

Richter, J., and Ullman, S. (1982). A model for the temporal organization of X- and Y-type receptive fields in the primate retina. *Biol. Cybern.* **43,** 127–145.

Ringach, D. L., Hawken, M. J., and Shapely, R. (1997). Dynamics of orientation tuning in macaque primary visual cortex. *Nature* **387** 281–284

Rockland, K. S., and Lund, J. S. (1982a). Intrinsic laminate lattice connection in primate visual cortex. *Science* **215,** 1532–1534.

Rockland, K. S., and Lund, J. S. (1982b). Widespread periodic intrinsic connections in the tree shrew visual cortex. *Brain Res.* **169,** 19–40.

Roerig, B., and Katz, L. C. (1998). Relationships of synaptic input patterns to orientation preference maps in ferret visual cortex. *Soc. Neurosci. Abstr.* **24,** 766.

Rodieck, R. W., and Stone, J. (1965). Analysis of receptive fields of cat retinal ganglion cells. *J. Neurophysiol.* **28,** 833–849.

Roig, B. R., Kabara, J. F., Snider, R. K., and Bonds, A. B. (1996). Non-uniform influence from stimuli outside the classical receptive field on gain control of cat visual cortical neurons. *Invest. Opthalmol. Vis. Sci. Suppl.* **37,** 2198.

Rojer, A., and Schwartz, E. L. (1990). Cat and monkey cortical columnar patterns modeled by band-pass-filtered 2d white noise. *Biol. Cybern.* **62,** 381–391.

Salinas, E., and Abbott, L. F. (1996). A model of multiplicative neural responses in parietal cortex. *Proc. Natl. Acad. Sci. U.S.A.* **93,** 11956–11961.

Sanchez-Vives, M. V., Nowak, L. G., McCormick, D. A. (2000). Membrane mechanisms underlying contrast adaptation in cat area 17 in vivo. *J. Neurosci.* **20,** 4267–4285.

Saul, A. B., and Cynader, M. S. (1989). Adaptation in single units in visual cortex: the tuning of aftereffects in the spatial domain. *Vis. Neurosci.* **2,** 593.

Sceniak, M. P., Ringach, D. L., Hawken, M. J., and Shapley, R. (1999). Contrast's effect on spatial summation by macaque V1 neurons. *Nat. Neurosci.* **2,** 733–739.

Schiller, P. (1982). Central connections of the retinal ON and OFF pathways. *Nature* **297,** 580–583.

Sclar, G., and Freeman, R. D. (1982). Orientation selectivity in the cat's striate cortex is invariant with stimulus contrast. *Exp. Brain Res.* **46,** 457–461.

Sengpiel, F., Sen, A., and Blakemore, C. (1997). Characteristics of surround inhibition in cat area 17. *Exp. Brain Res.* **116,** 216–228.

Sengpiel, F., Baddeley, R. J., Freeman, T. C. B., Harrad, R., and Blakemore, C. (1998). Different mechanisms underlie three inhibitory phenomena in cat area 17. *Vis. Res.* **8,** 2067–2080.

Shadlen, M., and Newsome, W. (1994). Noise, neural codes and cortical organization. *Curr. Opin. Neurobiol.* **4,** 569–579.

Sherk, H., and Horton, J. C. (1984). Receptive field properties in the cat's area 17 in the absence of on-center geniculate input. *J. Neurosci.* **4,** 381–393.

Sheth, B. R., Sharma J., Rao, S. C., and Sur, M. (1996). Orientation maps of subjective contours in visual cortex. *Science* **274,** 2110–2115.

Shoham, D., Glaser, D. E., Arieli, A., Kenet, T., Wijnbergen, C., Toledo, Y., Hidersheim, R., and Grinvald, A. (1999). Imaging cortical dynamics at high spatial and temporal resolution with novel blue voltage-sensitive dyes. *Neuron* **24,** 791–802.

Shou, T., Softky, W. R., and Koch, C. (1993). The highly irregular firing of cortical cells is inconsistent with temporal integration of random EPSPs. *J. Neurosci.* **13,** 334–450.

Sik, A., Penttonen, M., Ylinen, A., and Buzsaki, G. (1995). Hippocampal CA1 interneurons: an in vivo intracellular labeling study. *J. Neurosci.* **15,** 6651–6665.

Sillito, A. M. (1975). The contribution of inhibitory mechanisms to the receptive field properties of neurones in the striate cortex of the cat. *J. Physiol.* **250,** 305–329.

Sillito, A. M., Grieve, K. L., Jones, H. E., Cudeiro, J., and Davis J. (1995). Visual cortical mechanisms deetcting focal orientation discontinuities. *Nature* **378,** 492–496.

Sillito, A. M., Kemp, J. A., Milson, J. A., and Berardi, N. (1980). A re-evaluation of the mechanisms underlying simple cell orientation selectivity. *Brain Res.* **194,** 517–520.

Soodak, R. E., Shapley, R. M., and Kaplan, E. (1987). Linear mechanism of orientation tuning in the retina and lateral geniculate nucleus of the cat. *J. Neurophysiol.* **58,** 267–275.

Somers, D. C., Nelson, S. B., and Sur, M. (1995a). An emergent model of orientation selectivity in cat visual cortical simple cells. *J. Neurosci.* **15,** 5448–5465.

Somers, D. C., Toth, L. J., Todorov, E., Rao, S. C., Kim, D-S., Nelson, S. B., Siapas, A. G., and Sur, M. (1995b). Variable gain control in local cortical circuitry supports context-dependent modulation by long-range connections. In: Lateral interactions in the cortex: structure and function (J. Sirosh, R. Miikkulainen, and Y. Choe, Eds.), Austin, Univ of Texas Press. WWW electronic book, *http://www.cs.utexas.edu/users/nn/web-pubs/htmlbook96/somers/.*

Somers, D. C., Todorov, E. V., Siapas, A. G., Toth, L. J., Kim, D. S., and Sur, M. (1998). A local circuit approach to understanding integration of long-range inputs in primary visual cortex. *Cerebral Cortex* **8,** 204–217.

Sompolinsky, H., and Shapley, R. (1997). New perspectives on the mechanisms for orientation tuning. *Curr. Opin. Neurobiol.* **7,** 514–522.

Stemmler, M., Usher, M., and Niebur, E. (1995). Lateral interactions in primary visual cortex: a model bridging physiology and psychophysics. *Science* **269,** 1877–1880.

Stratford, K. J., Tarcky-Hornoch, K., Martin, K. A. C., Bannister, N. J., and Jack, J. J. (1996). Excitatory synaptic inputs to spiny stellate cells in cat visual cortex. *Nature* **382,** 258–261.

Suarez, H., Koch, C., and Douglas, R. (1995). Modeling direction selectivity of simple cells in striate visual cortex within the framework of the canonical microcircuit. *J. Neurosci.* **15,** 6700–6719.

Swindale, N. V. (1992). A model for the coordinated development of columnar systems in primate striate cortex. *Biol. Cybern.* **66,** 217–230.

Thomson, A. M., and Deuchars, J. (1994). Temporal and spatial properties of local circuits in neocortex. *Trends Neurosci.* **17,** 119–126.

Thomson, A. M., and Deuchars, J. (1997). Synaptic interactions in neocortical local circuits: dual intracellular recordings in vitro. *Cerebral Cortex* **7,** 511–522.

Thomson, A. M., Deuchars, J., and West, D. C. (1993a). Large, deep layer pyramid-pyramid single axon EPSPs in slices of rat motor cortex display paired pulse and frequency-dependent depression, mediated presynaptically and self-facilitation, mediated postsynaptically. *J. Neurophysiol.* **70,** 2354–2369.

Thomson, A. M., Deuchars, J., and West, D. C. (1993b). Single axon excitatory postsynaptic potentials in neocortical interneurons exhibit pronounced paired pulse facilitation. *Neuroscience* **54,** 347–360.

Thomson, A. M., West, D. C., and Deuchars, J. (1995). Properties of single axon excitatory postsynaptic potentials elicited in spiny interneurons by action potentials in pyramidal neurons in slices of rat neocortex. *Neuroscience* **69,** 727–738.

Thomson, A. M., and West, D. C. (1993). Fluctuations in pyramid-pyramid excitatory postsynaptic potentials modified by presynaptic firing pattern and postsynaptic membrane potential using paired intracellular recordings in rat neocortex. *Neuroscience* **54,** 329–346.

Todorov, E. V., Siapas, A. G., and Somers, D. C. (1997a). A model of recurrent interactions in primary visual cortex. In: Advances in neural information processing systems, Vol. 9 (M. C. Mozer, M. I. Jordan, and T. Petsche, Eds.), pp. 118–124. Cambridge, MIT Press.

Todorov, E. V., Siapas, A. G., Somers, D. C., and Nelson, S. B. (1997b). Modeling visual cortical contrast adaptation effects. In: Computational neuroscience: trends in research 1997 (J. M. Bower, Ed.), pp. 525–531. New York, Plenum Press.

Tolhurst, D. J., and Dean, A. F. (1987). Spatial summation by simple cells in the striate cortex of the cat. *Exp. Brain Res.* **66,** 607–620.

Tolhurst, D. J., and Dean, A. F. (1990). The effects of contrast on the linearity of spatial summation of simple cells in the cat's striate cortex. *Exp. Brain Res.* **79,** 582–588.

Toth, L. J., Rao, S. C., Kim, D-S., Somers, D., and Sur, M. (1996). Subthreshold facilitation and suppression in primary visual cortex revealed by intrinsic signal imaging. *Proc. Natl. Acad. Sci. U.S.A.* **93,** 9869–9874.

Toth, L. J., Kim, D-S., Rao, S. C., and Sur, M. (1997a). Integration of local inputs in visual cortex. *Cerebral Cortex* **7,** 703–710.

Toth, K., Freund, T. F., and Miles, R. (1997b). Disinhibition of rat hippocampal pyramidal cells by GABAergic afferents from the septum. *J. Physiol.* **500,** 463–474.

Toyama, K., Kimura, M., and Tanaka, K. (1981). Organization of cat visual cortex as investigated by cross-correlation technique. *J. Neurophysiol.* **46,** 202–214.

Traub, R. D., and Miles, R. (1991). *Neuronal networks of the hippocampus.* Cambridge, Cambridge University Press.

T'so, D. Y., Gilbert, C. D., and Wiesel, T. N. (1986). Relationship between horizontal interactions and functional architecture in cat striate cortex as revealed by cross-correlation analysis. *J. Neurosci.* **6,** 1160–1170.

Troyer, T. W., Krukowski, A., Priebe, N. J., and Miller, K. D. (1998). Contrast-invariant orientation tuning in cat visual cortex: feedforward-tuning and correlation-based intracortical connectivity. *J. Neurosci.* **18,** 5908–5927.

Tsodyks, M. V., and Markram, H. (1997). The neural code between pyramidal neurons depends on neurotransmitter release probability. *Proc. Natl. Acad. Sci. U.S.A.* **94,** 719–723.

Tsumoto, T., Eckart, W., and Creutzfeldt, O. D. (1979). Modification of orientation sensitivity of cat visual cortex neurons by removal of GABA—mediated inhibition. *Exp. Brain Res.* **34,** 351–363.

Tucker, T. R., and Katz, L. C. (1998). Organization of excitatory and inhibitory connections in layer 4 of ferret visual cortex. *Soc. Neurosci. Abstr.* **24,** 1756.

Vidyasagar, T. R., and Urbas, J. V. (1982). Orientation sensitivity of cat LGN neurones with and without inputs from visual cortical areas 17, 18. *Exp. Brain Res.* **46,** 157–169.

Vogels, R., and Orban, G. A. (1991). Quantitative study of striate single unit responses in monkeys performing an orientation discrimination task. *Exp. Brain Res.* **84,** 1–11.

Volgushev, M., Vidyasagar, T. R., and Pei, X. (1995). Dynamics of the orientation tuning of postsynaptic potentials in the cat visual cortex. *Vis. Neurosci.,* **12,** 621–628..

Volgushev, M., Vidyasagar, T. R., and Pei, X. (1997). A linear model fails to predict orientation selectivity of cells in the cat visual cortex. *J. Physiol. (Lond)* **496,** 597–606.

Watkins, D. W., and Berkley, M. A. (1974). The orientation selectivity of single neurons in cat striate cortex. *Exp. Brain Res.* **19,** 433–446.

Wehmeier, U., Dong, D., Koch, C., and Van Essen, D. (1989). Modeling the visual system. In: Methods in neuronal modeling (C. Koch, and I. Segev, Eds.), pp. 335–359. Cambridge, MIT Press.

Weliky, M., Kandler, K., Fitzpatrick, D., and Katz, L. C. (1995). Patterns of excitation and inhibition evoked by horizontal connections in visual cortex share a common relationship to orientation columns. *Neuron* **15,** 541–552.

Weliky, M., and Katz, L. C. (1994). Functional mapping of horizontal connections in developing ferret visual cortex: experiments and modeling. *J. Neurosci.* **14,** 7291–7305.

Wilson, H. R., and Cowan, J. D. (1972). Excitatory and inhibitory interactions in localized populations of model neurons. *Biophys. J.* **12,** 1–24.

Worgotter, F., and Koch, C. (1991). A detailed model of the primary visual pathway in the cat: comparison of afferent excitatory and intracortical inhibitory connection schemes for orientation selectivity. *J. Neurosci.* **11,** 1959–1979.